NASA TECHNICAL
MEMORANDUM

NASA TM X- 64967

SPACE SHUTTLE SOLID ROCKET BOOSTER (SRB) SEPARATION

By Donald D. Tomlin
Systems Dynamics Laboratory

November 1975

NASA

George C. Marshall Space Flight Center
Marshall Space Flight Center, Alabama

1. REPORT NO. NASA TM X- 64967	2. GOVERNMENT ACCESSION NO.	3. RECIPIENT'S CATALOG NO.
4. TITLE AND SUBTITLE Space Shuttle Solid Rocket Booster (SRB) Separation		5. REPORT DATE November 1975
		6. PERFORMING ORGANIZATION CODE
7. AUTHOR(S) Donald D. Tomlin		8. PERFORMING ORGANIZATION REPORT #
9. PERFORMING ORGANIZATION NAME AND ADDRESS George C. Marshall Space Flight Center Marshall Space Flight Center, Alabama 35812		10. WORK UNIT NO.
		11. CONTRACT OR GRANT NO.
		13. TYPE OF REPORT & PERIOD COVERED
12. SPONSORING AGENCY NAME AND ADDRESS National Aeronautics and Space Administration Washington, D.C. 20546		Technical Memorandum
		14. SPONSORING AGENCY CODE

15. SUPPLEMENTARY NOTES

Prepared by Systems Dynamics Laboratory, Science and Engineering

16. ABSTRACT

This report presents a description of the system which is used to separate the solid rocket boosters from the Space Shuttle after they have expended most of their propellant and their thrust is near burnout. The dynamics of the separation are simulated in a computer program so that the separation system can be analyzed. The assumptions and ground rules used in analyzing this system are explained and the method of analysis is delineated. The capability of the separation system is presented together with data which may be used to aid in the design of the external tank and solid rocket booster interface. The results of a parameter study to determine the sensitivity of the separation to the initial state of the Space Shuttle are also presented.

17. KEY WORDS	18. DISTRIBUTION STATEMENT

19. SECURITY CLASSIF. (of this report) Unclassified	20. SECURITY CLASSIF. (of this page) Unclassified	21. NO. OF PAGES 65	22. PRICE

TABLE OF CONTENTS

LIST OF ILLUSTRATIONS

LIST OF ILLUSTRATIONS (Concluded)

LIST OF TABLES

LIST OF SYMBOLS AND MNEMONICS

<u>Symbol</u>	<u>Definition</u>
BSM	booster separation motor
c.g.	center of gravity
deg	degrees
deg/s	degrees per second
EAT	end of action time
ET	external tank
EWAT	end of web action time
ft	feet
ft/s	feet per second
FWD	forward
g	acceleration of gravity (32.2 ft/s^2)
I.C.	initial condition, vehicle state
in.	inches
ISOL	isolated or free-stream aerodynamics
lb	pounds
LSRB	left solid rocket booster
OET	Orbiter with external tank
P	roll rate
PROX	proximity aerodynamics

LIST OF SYMBOLS AND MNEMONICS (Concluded)

Symbol	Definition
psia	pounds per square inch absolute
Q	pitch rate
$\bar{Q}$	dynamic pressure
R	yaw rate
RSRB	right solid rocket booster
s	seconds
sgn	takes on the sign of the parameter
SRB	solid rocket booster
SSME	Space Shuttle main engine
WAT	web action time
α	angle of attack
β	angle of slide slip
δ	engine gimbal angle

TECHNICAL MEMORANDUM X-64967

SPACE SHUTTLE SOLID ROCKET BOOSTER (SRB) SEPARATION

I. INTRODUCTION

The Shuttle SRB's are separated from the Orbiter/External Tank (OET) after their thrust-to-weight becomes less than that of the OET with one SSME out. They are attached to the external tank (ET) at one point on the forward end and at three points on the aft end. The forward attach point is used to transfer the thrust force from the SRB to the ET and, at separation, requires the severing of only one bolt for the SRB to separate. The aft attach points consist of three struts which require the severing of three bolts (one in each strut) to separate. Simultaneously with the severing of the bolts, a signal to fire eight booster separation motors (BSM's) on each SRB is given. Four BSM's are located in the forward frustum of the SRB and four on the aft skirt (Fig. 1). These BSM's cause the SRB's to move radially away from the ET so that the Orbiter thrust can accelerate the OET axially away from the SRB's.

The SRB separation is complicated by several factors. Since a rocket is coming off each side, the Orbiter cannot make a maneuver to the side to aid the separation. Consequently, the Orbiter simply flies in an attitude-hold mode. This leaves the BSM's to move the SRB's out from the ET and down from the Orbiter's wing while the Orbiter engines move the Orbiter forward of the SRB's. However, the Orbiter engines are significantly above the OET c.g. The SSME cant for moment balance causes the OET to move (in the z-direction) toward the SRB's. The BSM must have sufficient thrust-down so that the SRB's will stay below (with respect to pilot orientation) the Orbiter wing until the greater axial acceleration of the OET puts the SRB's behind the Orbiter.

The OET is aerodynamically stable but the SRB's are unstable; consequently, the aerodynamics cause opposite moments on the bodies which causes them to rotate into each other. The aerodynamics are complicated by the bodies being in close proximity and thus a seven-way interpolation (two of which are performed by a single-slope value) is required. Since the OET has a 0.9 g $(g = 32.2 \text{ ft/s}^2)$ acceleration at nominal separation, the OET does not move away from the SRB quickly. Also, the SRB thrust decay is long which results in some residual thrust at separation and further lengthens the time for the SRB to separate.

The purpose of this document is to record the simulation procedures and the results of an evaluation of the SRB separation system. The strengths and weaknesses of the system and the analysis techniques are explained to yield a better understanding of the separation. Also, information which may be used as an input to the design of the SRB/ET interfaces and as an input to recovery studies is presented. The results shown herein were obtained in conjunction with the Northrop Services Corporation through the efforts of Mr. R. S. Laurens.

The analysis of the separation system capability showed that the system is adequate even with a BSM out. The results of the study of the sensitivity to variations of the separation initial conditions showed that the separation clearances were sensitive to angle of side slip. Side-slip values which were only slightly greater than the design initial conditions caused impacts. The separation was quite tolerant to large values of angle of attack and roll rate.

II. ASSUMPTIONS AND GROUND RULES

This analysis is based on Shuttle Configuration 5 geometry and mass properties which were current at the time of the writing of this document. Since Mission 3A causes the most severe separation initial conditions of the design missions, its trajectory parameters were used to initialize the separation simulations of this study. This mission is the launch of the Shuttle from Vandenberg Air Force Base to a 104 deg inclined orbit.

A. Separation Sequence

The separation sequence [1] is initiated when the internal pressure of both SRB's is sensed to be 50 psia. The pressure transducers have a tolerance of ±15 psia. An accelerometer which senses the reduced acceleration due to SRB thrust decay is used as a backup cue to initiate the separation sequence if the primary cue fails. Separation does not occur immediately following this cue, but the following separation sequence is currently performed:

    1. Cue + 0.8 s:

        a. SRB TVC is commanded to null.

        b. Orbiter control logic is changed to the logic used during second stage flight.

c. Attitude reference is revised to the existing attitude so that the attitude errors are set to zero at that moment. This revised attitude reference is held throughout the remainder of the separation event.

2. Cue + 2.5 s:

   BSM and pyrotechnics to effect physical separation are commanded to fire simultaneously (within specified tolerances).

3. Cue + 6.5 s:

   Reset to normal attitude reference.

Two separate computer programs are used by MSFC for separation analysis. An ascent computer program is used to establish the initial conditions for separation. It simulates Shuttle flight until the SRB's are physically separated. The separation computer program takes over from that point and simulates the Shuttle and the two individual SRB flights until the SRB's have no chance of recontacting the OET.

B. Booster Separation Motors (BSM's)

Sixteen separation motors are used on each Shuttle flight (eight on each SRB). Four motors are located in the forward frustum and four are on the exterior of the aft skirt. The orientation of the BSM's is shown in Figure 1. The aft motors are located unsymmetrically which causes a small roll moment. The BSM's resultant total thrust vector can be misaligned [1] as much as 1 deg on the 20 deg angle shown in Figure 1 and 2 deg on the 40 deg angle. An analysis of these misalignments was performed, as reported in reference 2, which showed that angles of 19 deg and 42 deg produced the least clearance. Consequently, these angles were used in the subsequent simulation in place of the 20 deg and 40 deg angles shown in Figure 1.

The BSM minimum performance is given in Reference 1 and was used in this analysis. Since the separation performance is dependent upon the performance of four BSM's at each location, the performance specification is given in terms of four motors as follows:

1. The average thrust-over-the-web action time shall be greater than or equal to 74 000 lb.

2. Initial thrust following the ignition transient shall be greater than or equal to the average web action thrust.

3. Total impulse over the web action time shall be greater than or equal to 56 000 lb-s.

4. Total impulse over the action time shall be greater than or equal to 60 000 lb-s.

5. Thrust rise to 90 percent of average thrust shall be within 47 to 137 ms of ignition command.

6. Time from end-of-web-action-time (EWAT) to the time that thrust is one-half the thrust of EWAT shall be less than or equal to 0.1 s.

7. Web action time shall be less than or equal to 0.8 s.

Figure 2 shows this specification for four motors as we have interpreted it. The minimum values were used in all cases to produce conservative results. Instead of having a long thrust rise time, a long ignition delay was used to obtain these results.

C. Separation Clearance

The BSM's orientation and locations are such that they cause the SRB's to move down and out relative to the pilot orientation. Also, the nose of the SRB rotates down relative to the pilot. However, the primary relative motion of the SRB is rearward which is caused by the Orbiter's greater axial acceleration moving the OET forward. With these expected movements of the SRB relative to the OET, certain areas were considered to have a greater likelihood of recontact.

The separation simulation program has a routine to determine the minimum clearance between the skin of the SRB and the exterior insulation on the skin of the ET. It also determines where the minimum clearance exists on the SRB and ET. The ET aft dome is modeled as a hemispherical dome which gives some conservatism to the analysis (Fig. 3).

The forward attach structure (Fig. 4) has an initial 1 in. clearance between ET attach structure and the SRB skin; consequently, this clearance is tracked in the computer program. Also, the SRB forward attach structure is

4

tracked with respect to skin on the ET. The exterior insulation on the ET, which is 1 in. thick, has not been taken into account so that the clearances should be reduced by 1 in. The electrical connection shown in Figure 4 is not a problem because the SRB moves in the z-direction which moves the bracket out of the way.

The aft attach struts are shown in Figure 5. Since the ET external insulation is not shown, the clearance is 1 in. less than that shown in the figure. The SRB moves back and down primarily. Because of this motion, the SRB ring and strut stubs are behind the ET before they can approach the ET insulation; consequently, it is not important to check these for clearance. Also, the upper strut stubs of the ET are not checked for clearance because the SRB moves down (in relation to the pilot's orientation). However, the bottom ET strut stub is checked for clearance of the SRB skin because the SRB's move down toward them. The strut stub is modeled as a spherical surface section because it has some freedom to pivot at the swivel pin joint.

In summary, the clearances that are checked are (1) the skin-to-skin of the ET and SRB, (2) the forward attach points to ET and SRB skins, and (3) the aft bottom ET strut stub to SRB skin.

D. Aerodynamics

During the time the BSM's are firing, their plumes disturb the aerodynamic flow field. To accurately simulate the separation during this time, the aerodynamic data are based on wind tunnel tests with simulated BSM plumes. After the BSM's have decayed, the aerodynamic data are based on wind tunnel tests with the BSM plumes off. Therefore, two sets of data are used in the separation simulation: plume-on and plume-off aerodynamic data. The plume-on aerodynamics are based on portions of wind tunnel test IA13 which had an OET and one SRB, the right-hand SRB. As explained elsewhere in this report, the data have been manipulated to take into account the presence of the left SRB (LSRB). Plumes simulated for this wind tunnel test were based on an early configuration of BSM orientation and location so that these simulations must be repeated for verification where more up-to-date plume-on wind tunnel test data become available. The plume-off aerodynamics are based on portions of wind tunnel tests IA13, IA57, and IA87.

E. SRB Thrust

The cue to separate is based on the SRB chamber pressure; i.e., physical separation occurs 2.5 s after the pressure in both the SRB's is below 50 ± 15 psi. The higher the SRB thrust at separation, the more difficult the separation is because the SRB does not fall back as quickly. Consequently, the separation cue was assumed to occur at 50 + 15 psi, and, 2.5 s later, the SRB thrust is approximately 30 000 lb. Therefore, the separation program initializes both SRB's thrusts at 30 000 lb and decays them nominally from that point.

Because of the characteristics of the SRB flexible seal, the SRB nozzle moves toward the exterior of the pressure chamber as the pressure increases in the SRB's. Since the actuators are located on the opposite side from the ET, the nozzles will cant outward from the ET as the pressure increases. It is planned to pre-cant the nozzles so that, during maximum dynamic pressure region of flight, the nozzles are aligned with the SRB centerline. This causes the nozzles to be canted in at separation and, at 0 psi pressure in the SRB, the inward cant is approximately 1 deg. This inward cant of the SRB's is deterministic and programmed versus internal pressure in the computer simulation.

F. Separation Initial Conditions (Vehicle States)

The vehicle states which have major effects on the ability of the separation system to separate the SRB without recontact are dynamic pressure $(\bar{Q})$, angle of attack (α), angle of side slip (β), roll rate (P), pitch rate (Q), yaw rate (R), and the SSME gimbal angles $(\delta_{zi}$ and $\delta_{yi})$. Reference 1 specifies that the separation system shall be capable of separating the SRB's from the OET when the vehicle has the state which is shown in Table 1 as the design initial conditions. The design initial conditions are used as the requirements for design of the separation system. The basis for setting these values was to be able to separate without delay from all ascent cases which could complete the mission. To do this, the largest individual design initial condition variables were selected from many ascent simulations that completed the mission without regard to the values of the other variables. For example, the largest value of roll rate was selected from all of the ascent simulations and the largest value of pitch rate was selected from all of the ascent simulations, but they are not necessarily from the same simulation. Consequently, all of the design initial condition variables form an envelope above those variables for the ascent simulations which could complete the mission. The magnitudes of the envelopes are sensitive to the design disturbances and to the control system configuration.

TABLE 1. SEPARATION INITIAL CONDITIONS

Parameter	Q	α	β	P	Q	R	δ_y/δ_z		
Units	psf	deg	deg	deg/s			deg		
Engine No.							1	2	3
Worst Case No Malfunction	70.1	3.3	-8.8	5	0.7	-0.6	-2.3/ -5.5	-7.6/ 2.5	3.1/ 2.5
Design	75	15	15	5	-2	-2	0/0	0/0	0/0
Nominal	59.3	0.8	-12.1	1.7	0.54	-0.02	-1.5/ -2.4	-3.6/ 0.7	+0.6/ 0.7

Control configurations are influenced by loads and performance as well as the end conditions of the SRB flight. The latest changes in control system design have been somewhat detrimental to the achievement of state variable envelopes which fit within the specified design initial conditions. Some of the ascent simulations involving a vehicle in sufficiently good condition for mission completion have shown roll rates in excess of 5 deg/s at the nominal separation time; however, the probability of this occurrence is very remote. The vehicle has an automatic inhibit which inhibits separation if any of the following design initial condition variables are exceeded: dynamic pressure, roll rate, pitch rate, and yaw rate. When these response variables are all within the design initial conditions, the inhibition is removed.

The design initial condition variables result from some simulations which include malfunctions. A set of initial conditions was needed to determine the capability of the separation system in the event one of the BSM's failed to fire. Since the design initial conditions already considered a failure, using those initial conditions for the BSM failure case would violate the program groundrules of not accommodating double failures. Rockwell International reviewed their ascent runs and designated one case as the "worst case no-malfunction" (Table 1) which could be used to determine the separation system's capability with a BSM failure.

III. RESULTS

This study was performed in support of the SRB and ET design activity and in support of Johnson Space Center and Rockwell International systems activities. While these results are not official design data, they are intended to provide supplemental data for element and system design.

A. Capability of the Separation System

The separation system is designed to separate the SRB's under design initial conditions (Table 1) without the SRB's colliding with any portion of the OET or without contacting each other. These results include "worst case" BSM misalignments and minimum performing BSM's. Also, a 0.125 s delay in ignition of the BSM is used to simulate the worst case BSM ignition delay and thrust rise time (Fig. 2). The picture plots of SRB separation with design initial conditions are shown in Figure 6. Since the movements of the SRB's are not continuously out and away from the OET, it is necessary to examine more closely those areas of possible contact. The minimum clearances of the forward attach points are shown in Figure 7. The ignition delay of the BSM's allows the clearance at attach points to decrease before increasing. Figure 8 gives the minimum clearances between the skins of the SRB's and ET and between the lower aft strut stub of the ET and the skin of the SRB's. The locations of the minimum skin-to-skin clearance are given in Figure 9. These locations are station numbers in the respective coordinate systems. Although some of the clearances are reduced significantly, there is no case of recontact. The separation system has been redesigned in the past because the BSM plume damaged the insulation on the Orbiter nose. Consequently. the BSM plume angle with the Orbiter nose and the distance between the BSM's and the Orbiter nose are monitored. Figure 10 shows the results for the design initial conditions. The BSM's start the thrust decay at 0.875 s; the minimum plume angle at that time is 42 deg on the LSRB. Although there is no requirement to separate the SRB's with a BSM failing to fire, it is highly desirable to have that capability. Therefore, cases where a BSM failed to fire were run. The forward BSM failure was found to be the most critical. The design initial conditions were not used because, to have initial conditions as severe as the design initial conditions, a failure must have occurred during ascent flight. Therefore, using the design initial conditions in conjunction with a BSM failure would constitute a double failure which does not need to be accommodated under the Shuttle program ground rules. Thus, the worst-case no-malfunction initial conditions (Table 1) were used. The picture plots are shown in Figure 11. The clearances are shown in Figures 12 and 13, and the location of the minimum skin-to-skin

clearances is shown in Figure 14. The lower rear strut on the ET comes to within 4 in. of the SRB skin before the clearance distance increases. The BSM plume angles and distances are given in Figure 15 and show a minimum angle of 44 deg at BSM thrust tailoff on the LSRB.

B. Output Data

Attach-point motions are given in Figures 16 through 19 for the nominal initial conditions (Table 1). These represent the nominally expected motions of the SRB side of the interfaces relative to the ET interfaces. The struts are assumed to be rigidly cantilevered from the SRB and ET. Since they have some rotational freedom, these relative motions will be somewhat in error. However, it is believed that these figures will be useful in the design of the SRB disconnects. Figures 20 through 23 contain the attach-point motions for the design initial condition which represent a diverse case from the nominal initial conditions.

The SRB states at 3 s after separation are given in Table 2. These states are for a Vandenburg Air Force Base launch. At approximately 3 s after separation, the aero-interference effects are small and free-stream aerodynamics may be used. The states for the nominal initial conditions represent the nominally expected values where those for the design initial condition represent a diverse case. These data may be helpful to those studying the recovery of the SRB.

C. Initial Condition Sensitivity

Several simulations were made to determine the sensitivity of the separation clearances to initial conditions at separation. The results are shown in Table 3. The dynamic pressure was varied while the initial conditions were the design initial conditions. The separation appears to be sensitive to the dynamic pressure but, when one considers the severity of the design initial conditions and the other parameters listed in the note in Table 3, it is realized that, normally, much higher dynamic pressures could be tolerated. Since no impacts were encountered at the large angles of attack of ±30 deg, it was established that separation was insensitive to angle of attack alone.

The separation is sensitive to angle of side slip. Slight increases above the design initial condition values resulted in impacts. The pitch and roll rates are not nearly as sensitive. The separation is sensitive to the lateral directional parameters but is relatively insensitive to the longitudinal parameters and roll rates.

TABLE 2. SRB CONDITIONS 3 s AFTER SEPARATION INITIATION

Parameter	Nominal IC		Design IC	
	RSRB	LSRB	RSRB	LSRB
X Position (ft)	21047610	21047605	21047613	21047593
Y Position (ft)	-5770.6	-5706.8	-7315.6	-7269.9
Z Position (ft)	320597.6	320599.1	320910	320892
X Inertial Vel. (ft/s)	2165.2	2165.3	2157.9	2152.4
Y Inertial Vel. (ft/s)	950.5	959.8	449.1	450.8
Z Inertial Vel. (ft/s)	5079.3	5079.5	5181.5	5181.5
ϕ (deg)	180.68	190.94	-179.31	-171.43
θ (deg)	-36.85	-40.08	-51.61	-45.40
Ψ (deg)	-8.24	1.93	33.63	37.60
p (deg/s)	-1.17	3.22	4.01	8.09
q (deg/s)	-11.96	-8.21	-7.94	-16.33
r (deg/s)	6.49	3.30	-9.36	-9.15
Latitude (deg)	28.4891	28.4889	28.4933	28.4932
Longitude (deg)	-80.1250	-80.1250	-80.1240	-80.1240
Altitude (ft)	140276	140271	140283	140263
Path Angle (deg)	30.41	30.39	30.30	30.23
Heading (deg)	105.06	105.20	97.39	97.42

	$\bar{Q}$ (psf)	α (deg)	β (deg)	p (deg/s)	q (deg/s)	r (deg/s)
Nominal IC	59.3	0.08	-12.1	1.7	0.54	-0.02
Design IC	75	-15	15	5	-2	-2

TABLE 3. INITIAL CONDITION SENSITIVITIES

Parameter	Units	No Impact Value	Impact Value	Where Impact Occurs	Comments
Dynamic Pressure, $\bar{Q}$	psf	90	100	Fwd. Attach	Design IC, $\delta_{eng} = 0$
Angle of Attack, α	deg	±30			Large α precluded further simulations
Angle of Side Slip, β	deg	±15	±20	Fwd. Attach	
Roll Rate, P	deg/s	±15			Large P precluded further simulations
Pitch Rate, Q	deg/s	-13	-15	Wing	Less sensitive to +Q
Yaw Rate, R	deg/s	±7	±8	Skin-to-skin	

NOTE: Except as noted above, the following is true of each case simulated: $\bar{Q}$ = 75 psf, α = β = 0 deg, P = Q = R = 0 deg/s, Orbiter engines initialized to initial conditions, BSM misalignments of 1 deg roll outward and 2 deg pitch toward the SRB centerline, 0.125 s BSM ignition delay.

D. Control Mode Modifications

The present procedure for control mode modification is to actively control the OET with the Orbiter SSME's during the separation of the SRB's. Sometimes, these control torques cause the OET to rotate toward the SRB's thus reducing the clearances. To determine if the clearances could be increased, the SSME's were commanded to null when separation occurred and, 1.5 s after separation, the control using these engines was ramped back in. Engine control

is needed prior to separation to damp out the body rates; therefore, the engines should not be at null upon initiating separation. The three cases of initial conditions given in Table 1 were used to test the hypothesis. A comparison between the nominal engine control cases and the cases where the SSME engines were nulled was made. Table 4 gives the clearance distances for eight critical points between the OET and SRB's. For the nominal initial conditions, there was no significant difference in the two cases but, for the worst-case no-malfunction initial conditions, the clearance for the aft lower-strut-to-RSRB-skin was greater in the case where the SSME's were nulled. For the design initial condition, the case with the SSME's nulled reduced the clearance for the aft lower-strut-to-RSRB-skin. With these conflicting results, changes in the OET separation procedure are not recommended. Also, Reference 3 points out the shortcoming of stage 2 control gains for separation. If the control gains are changed, it could change the results in this analysis and further investigations would be necessary to determine if this separation procedure change would be advantageous.

IV. CONCLUSIONS

The separation system has been tested against the severe design initial conditions. The separation will be inhibited if the dynamic pressure or any of the body rates exceed the values of the design initial conditions. Consequently, with the clearances given in Table 5, the separation system is capable of meeting the Shuttle requirements. In addition, the separation system was tested against the worst-case no-malfunction initial condition with a BSM out, and the clearances which are given in Table 5 demonstrate that the separation is satisfactory. The separation aerodynamics are complicated, and it is difficult and costly to perform accurate and sufficient wind tunnel testing. Therefore, some simplifications have been used at the expense of accurate data. The data uncertainty at this time is significant and could affect these conclusions. Future wind tunnel tests which are planned should reduce this uncertainty.

The data provided for the initial conditions to SRB recovery studies and for the attach-point motion may be used by the ET and SRB interface designers. Further data may be obtained by contacting the author.

The results of the study of the sensitivity to variation of the separation initial conditions showed that the separation clearances were sensitive to angle of side slip (Table 3). Separation initial condition values of this variable, which were only slightly greater than the design initial conditions, caused

TABLE 4. MINIMUM CLEARANCE DISTANCES (in.) FOR SRB SEPARATIONS
WITH AND WITHOUT SSME ENGINE CONTROL

Initial Conditions	SSME Control	LSRB Fwd* Attach to ET Skin	ET Fwd. Attach to LSRB Skin	RSRB Fwd Attach to ET Skin	ET Fwd. Attach to RSRB Skin	ET Skin to LSRB Skin	ET Skin to RSRB Skin	ET Aft LWR Strut to LSRB Skin	ET Aft LWR Strut to RSRB Skin
Nominal	Active	2.70	0.82	2.81	0.94	10.8	10.8	16.8	15.7
	Ramped Out	2.70	0.82	2.82	0.94	10.8	10.8	16.8	16.8
Worst-Case No-Malfunction	Active	2.88	1.0	2.86	1.0	10.9	10.6	16.8	5.1
	Ramped Out	2.87	1.0	2.87	1.0	10.9	10.7	16.8	14.2
Design	Active	2.74	0.86	2.19	0.29	10.4	10.2	11.2	5.5
	Ramped Out	2.74	0.86	2.22	0.29	10.5	10.2	9.6	1.4

*The ET skin has one inch of external insulation which reduces the stated clearance by one inch.

TABLE 5. MINIMUM SRB-ET CLEARANCE DISTANCES

Clearance Description	Worst Case No-Malfunction with Fwd BSM Out		Design Initial Conditions		Initial Clearance Distance (in.)
	Minimum Clearance Distance (in.)	Time of Minimum Clearance (s)	Minimum Clearance Distance (in.)	Time of Minimum Clearance (s)	
ET Fwd Attach to LSRB Skin	0.99	0.0625	0.849	0.1563	1.00
LSRB Fwd Attach to ET Insulation	1.880	0.0625	1.730	0.1563	1.88
ET Fwd Attach to RSRB Skin	0.992	0.1250	0.325	0.2188	1.00
RSRB Fwd Attach to ET Insulation	1.857	0.1250	1.216	0.2188	1.88
ET Skin to RSRB Skin	9.917	0.3438	10.274	0.2188	11.0
ET Skin to LSRB Skin	10.935	0.1250	10.626	0.2188	11.0
ET Aft Lower Strut to RSRB Skin	4.500	0.8125	4.136	0.6563	16.778
ET Aft Lower Strut to LSRB Skin	16.773	0.0	7.126	0.75	16.778

	$\overline{Q}$ (psf)	α (deg)	β (deg)	p (deg/s)	q (deg/s)	r (deg/s)
Worst-Case No-Malfunction IC	70.1	3.3	-8.8	5.0	0.7	-0.6
Design IC	75.0	15.0	15.0	5.0	-2.0	-2.0

14

impacts of the SRB. The other variables were less sensitive. Separation initial values of roll rate and angle of attack that were significantly greater than the design initial condition could be tolerated without an impact.

The ascent simulations, which included the thrust mismatch of Figure A-1 and snubber gimbal limiter of Figure A-2, have resulted in roll rates that exceed the design initial conditions. This exceedance would cause the staging of the SRB's to be delayed. Since the staging can be performed at roll rates greater than the design initial condition values, the staging delays could be eliminated by increasing the design initial condition value of the roll rate. Also, it was noted in the ascent simulations that, in second-stage control, the roll rates would be increased by the Orbiter engine. The cross-coupling of the Orbiter engines in trying to control yaw would cause the roll rate to increase. This could be corrected by increasing the roll gain and decreasing the yaw gain, or by simply continuing with first-stage control logic, while in the initial part of second-stage flight.
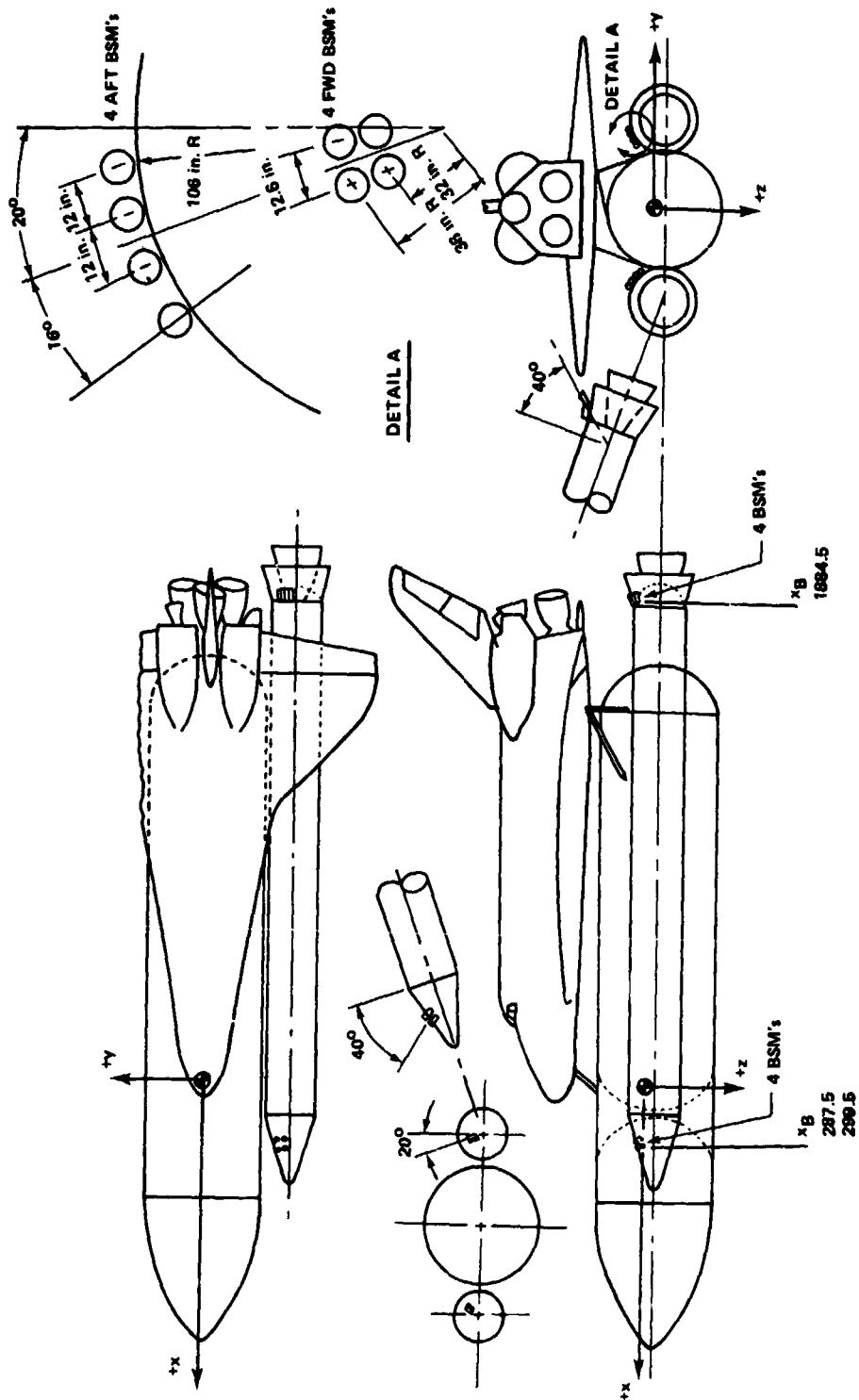
Figure 1. BSM location and attitudes.
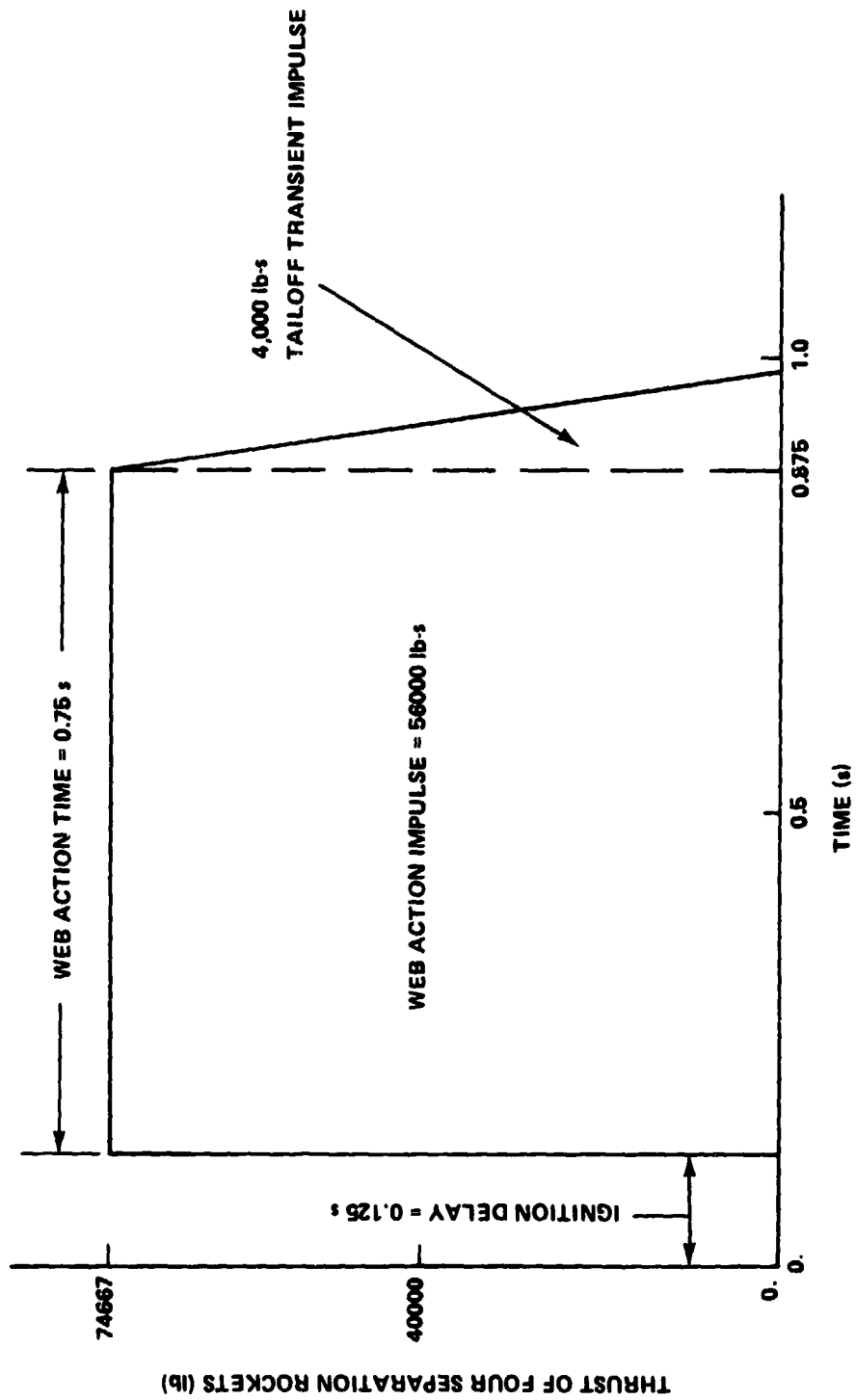
Figure 2. Modeling of BSM thrust characteristics.

17

OLD CYLINDRICAL MODELING

SPHERICAL MODELING

ACTUAL ET
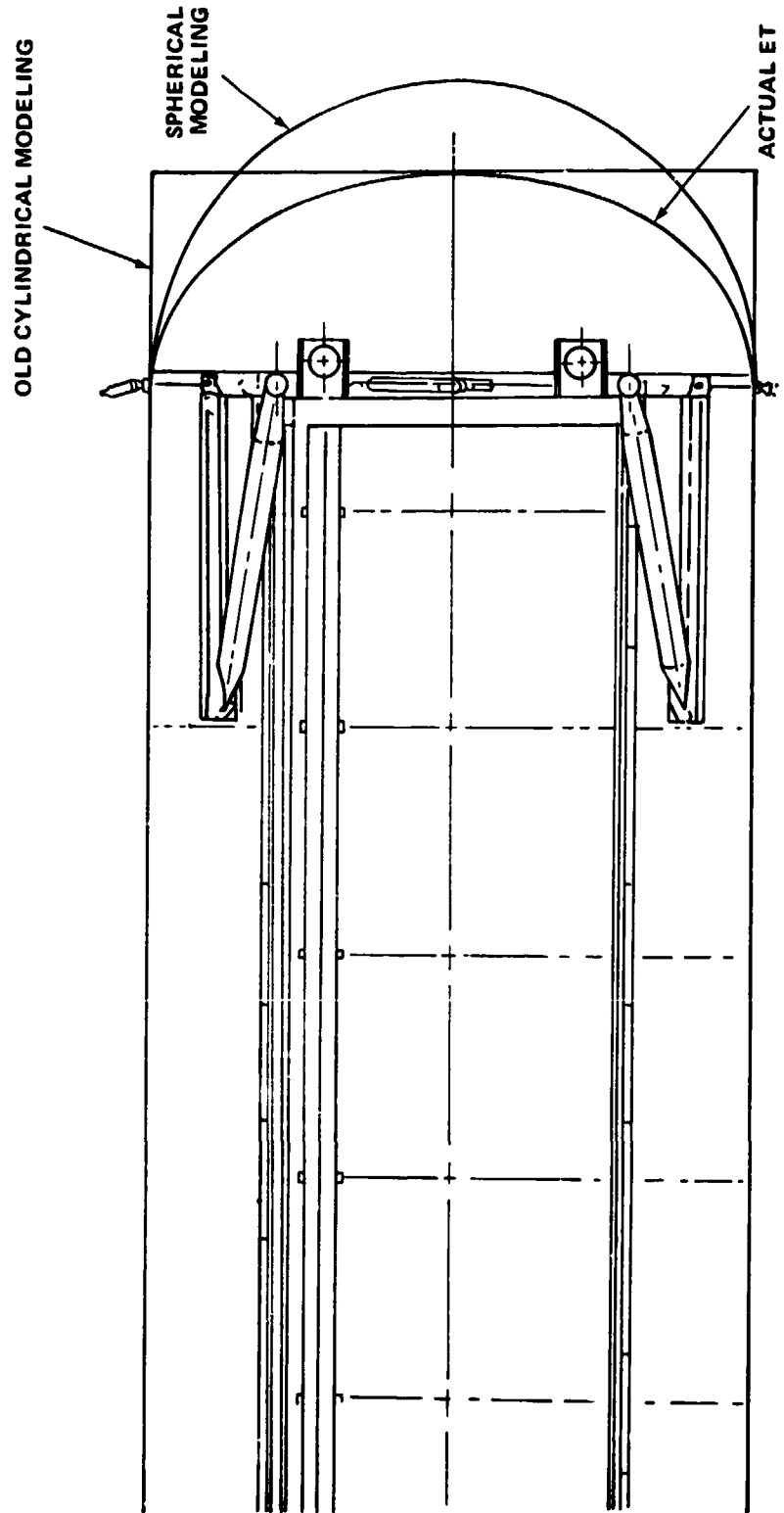
Figure 3. External tank modeling for impact routine.
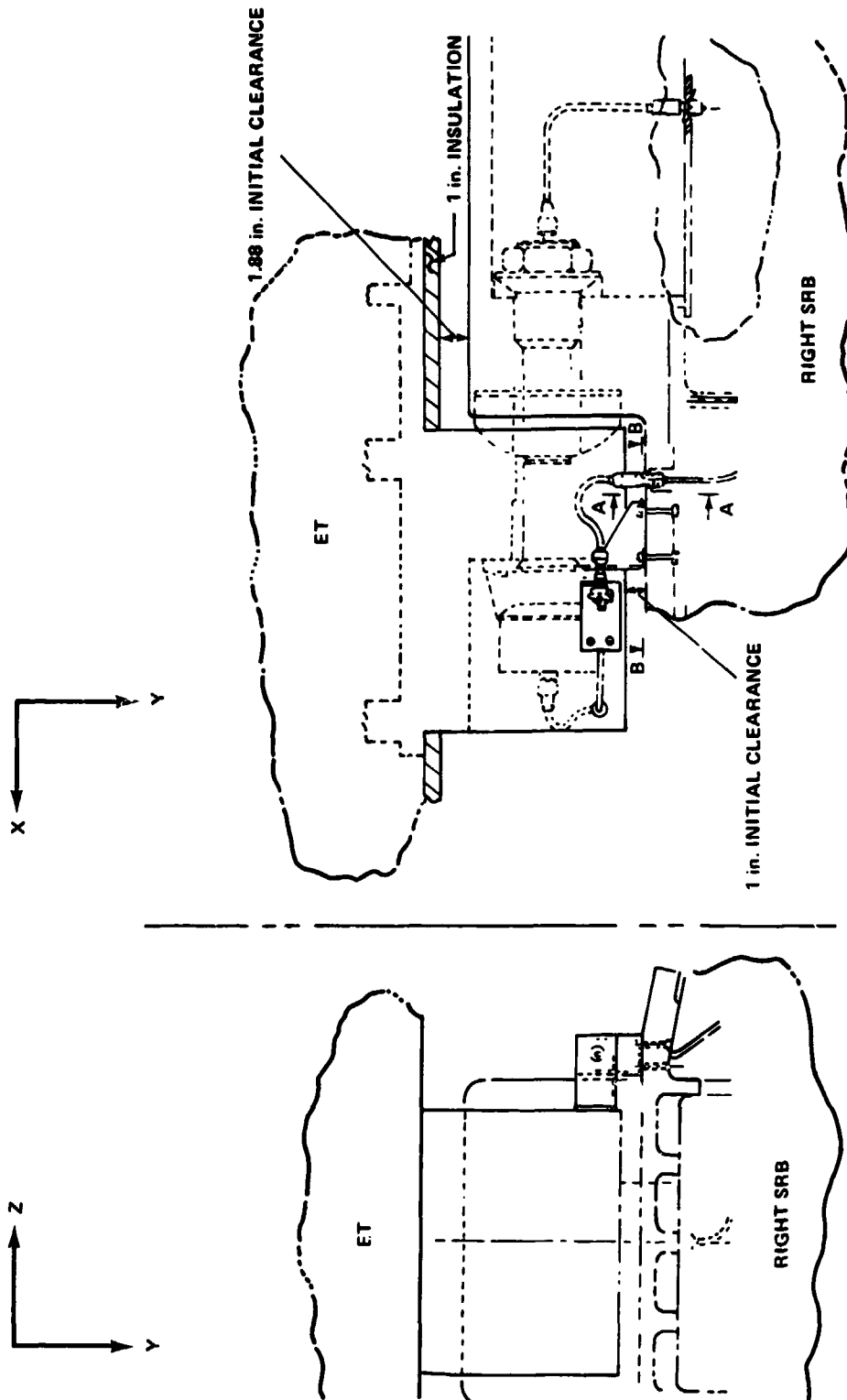
Figure 4. RSRB forward attach structure.

19
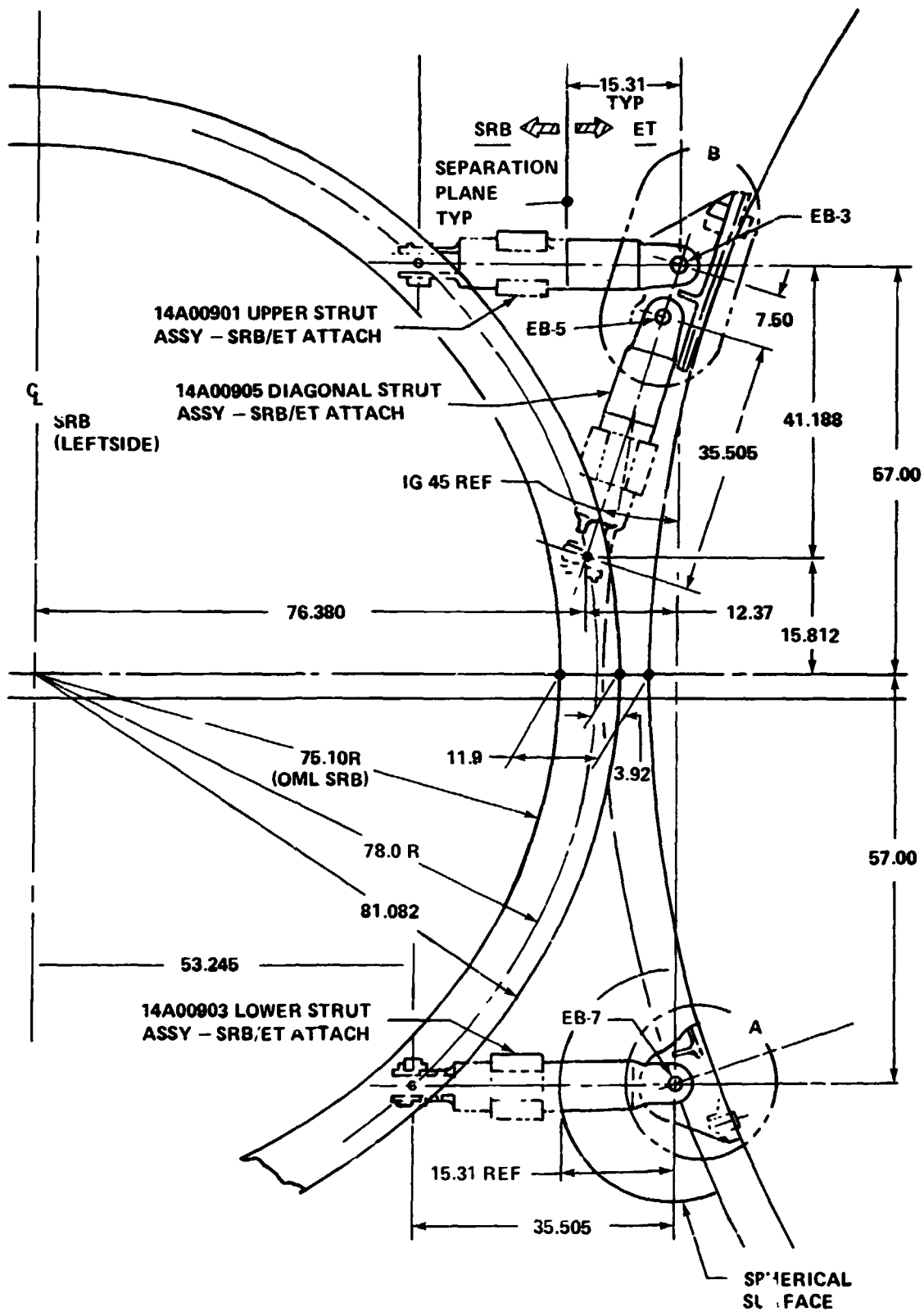
Figure 5. Aft attach struts.

20

BOTTOM VIEW
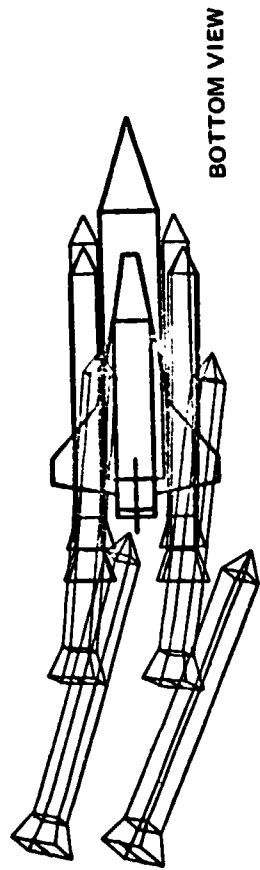
NOTE: Pictures shown in 1 sec. increments.

LEFT SIDE VIEW

REAR VIEW
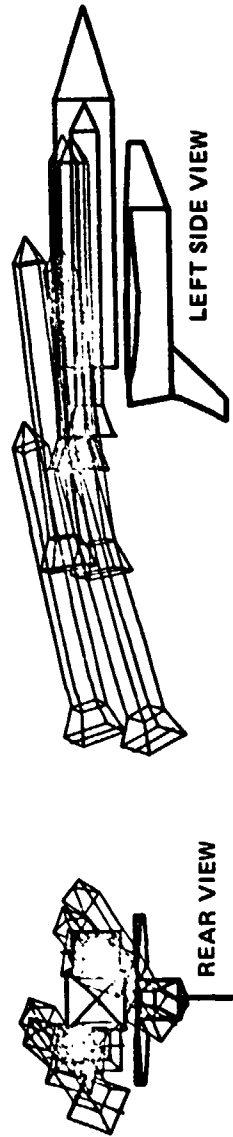
Figure 6. SRB separation for design initial conditions.
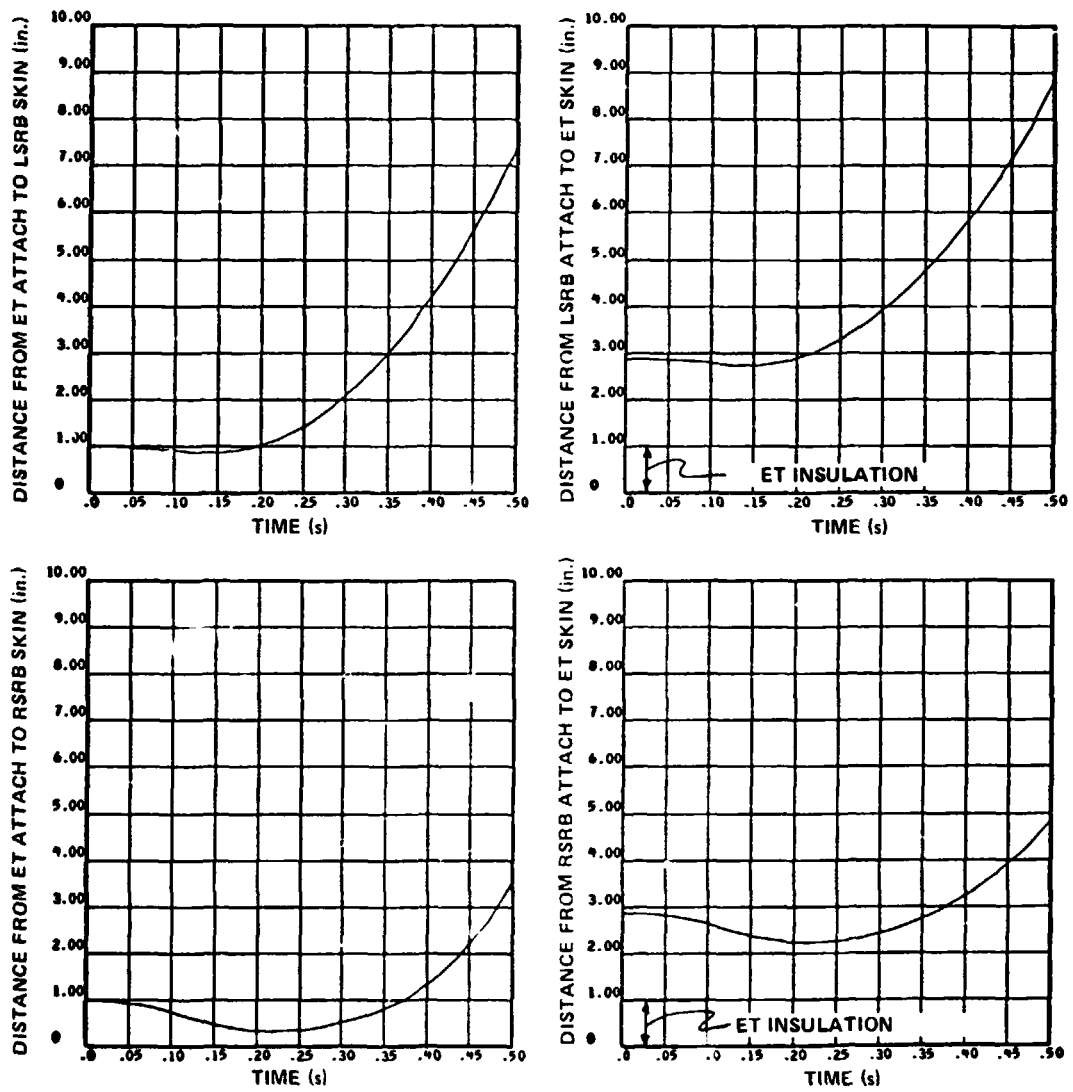
Figure 7. Separation clearances between SRB/ET forward attach structures for design initial conditions.
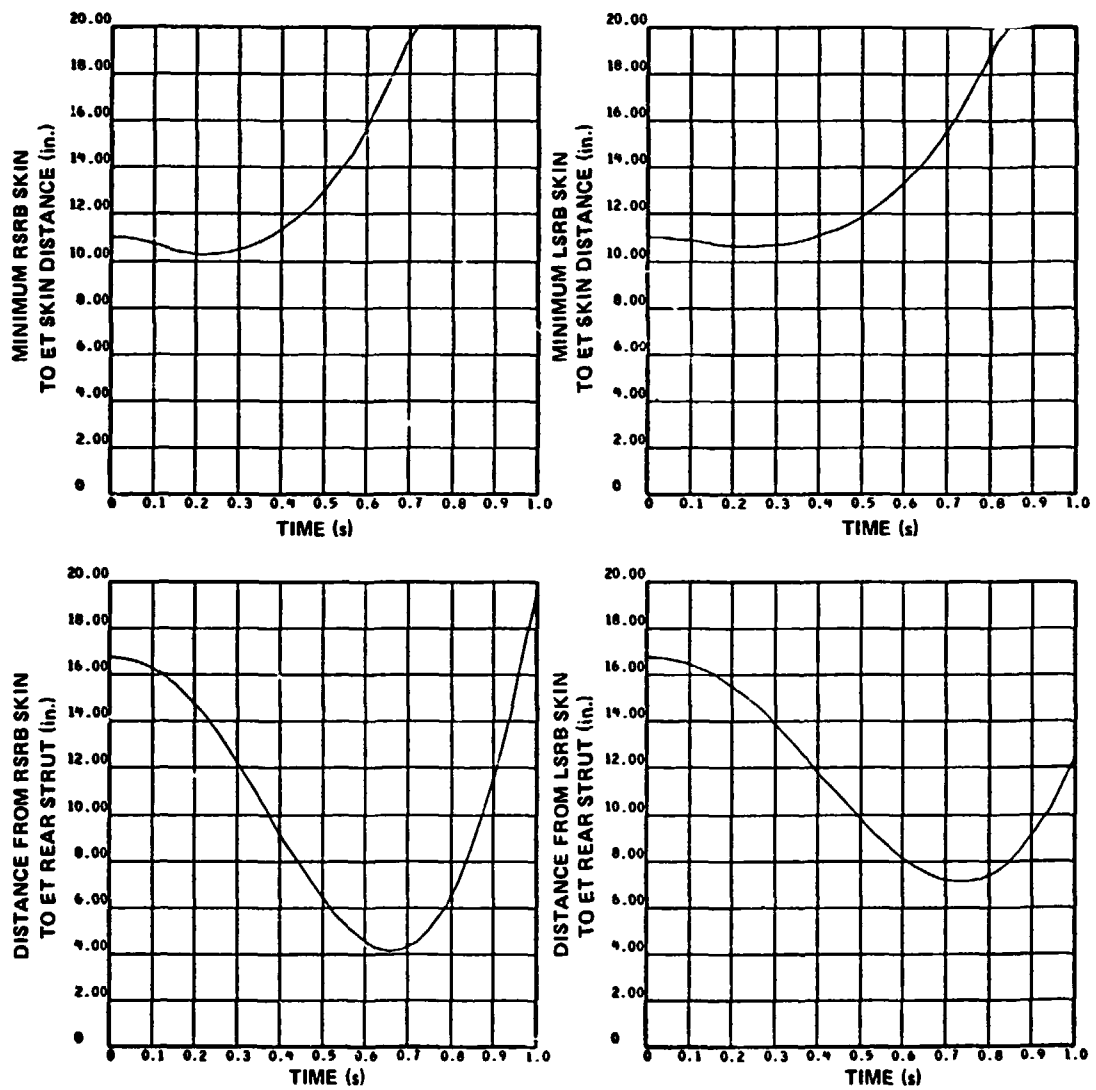
Figure 8. Separation clearances between SRB/ET skin-to-skin and rear struts for design initial conditions.
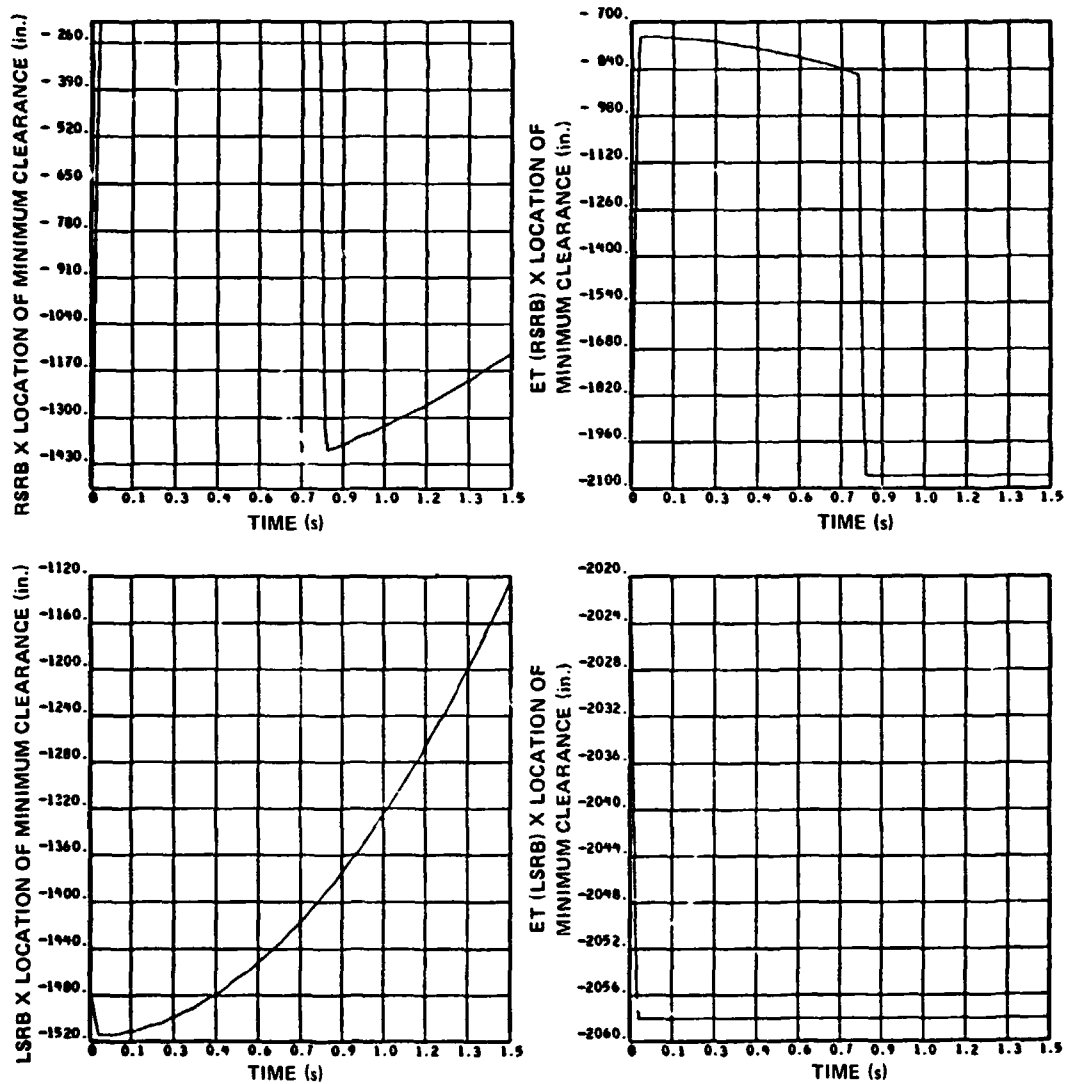
NOTE: SRB LOCATIONS ARE STATION NUMBERS IN THE SRB SYSTEM AND
ET LOCATIONS ARE STATION NUMBERS IN THE ET SYSTEM
(DISREGARD THE MINUS SIGNS).

Figure 9. Axial location of minimum skin-to-skin clearance
for design initial conditions.
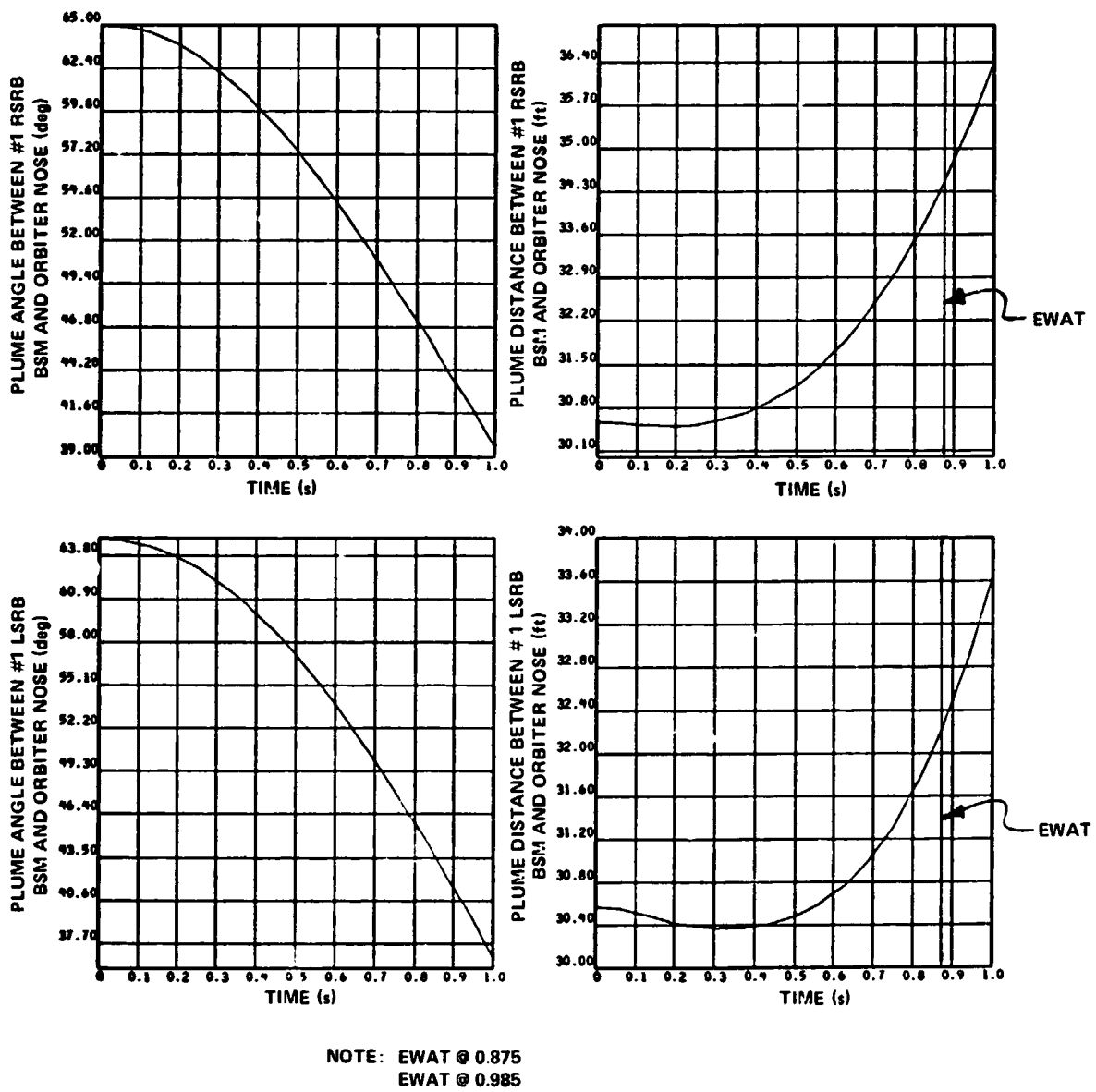
Figure 10. BSM #1 plume angle and distance to orbiter nose for design initial conditions.

BOTTOM VIEW
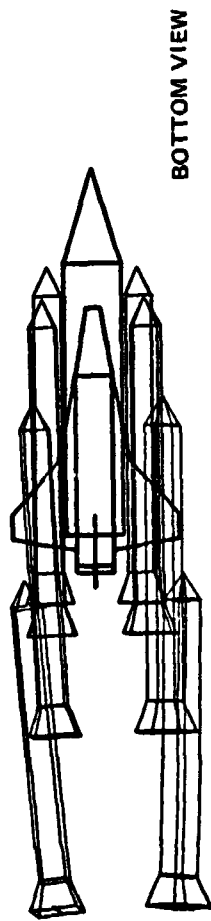
NOTE: PICTURE SHOWN IN 1 s INCREMENTS.

LEFT SIDE VIEW

REAR VIEW
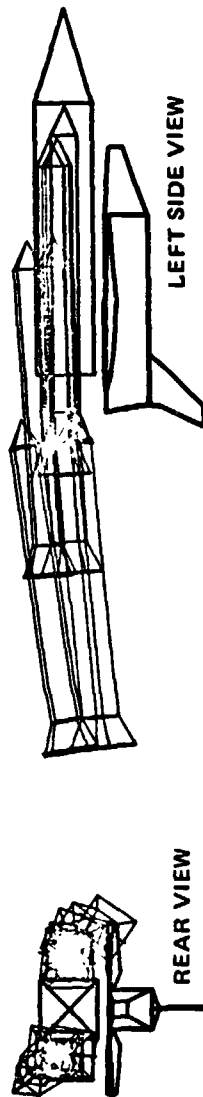
Figure 11. SRB separation for worst case no-malfunction initial conditions
and a forward BSM failed on each SRB.
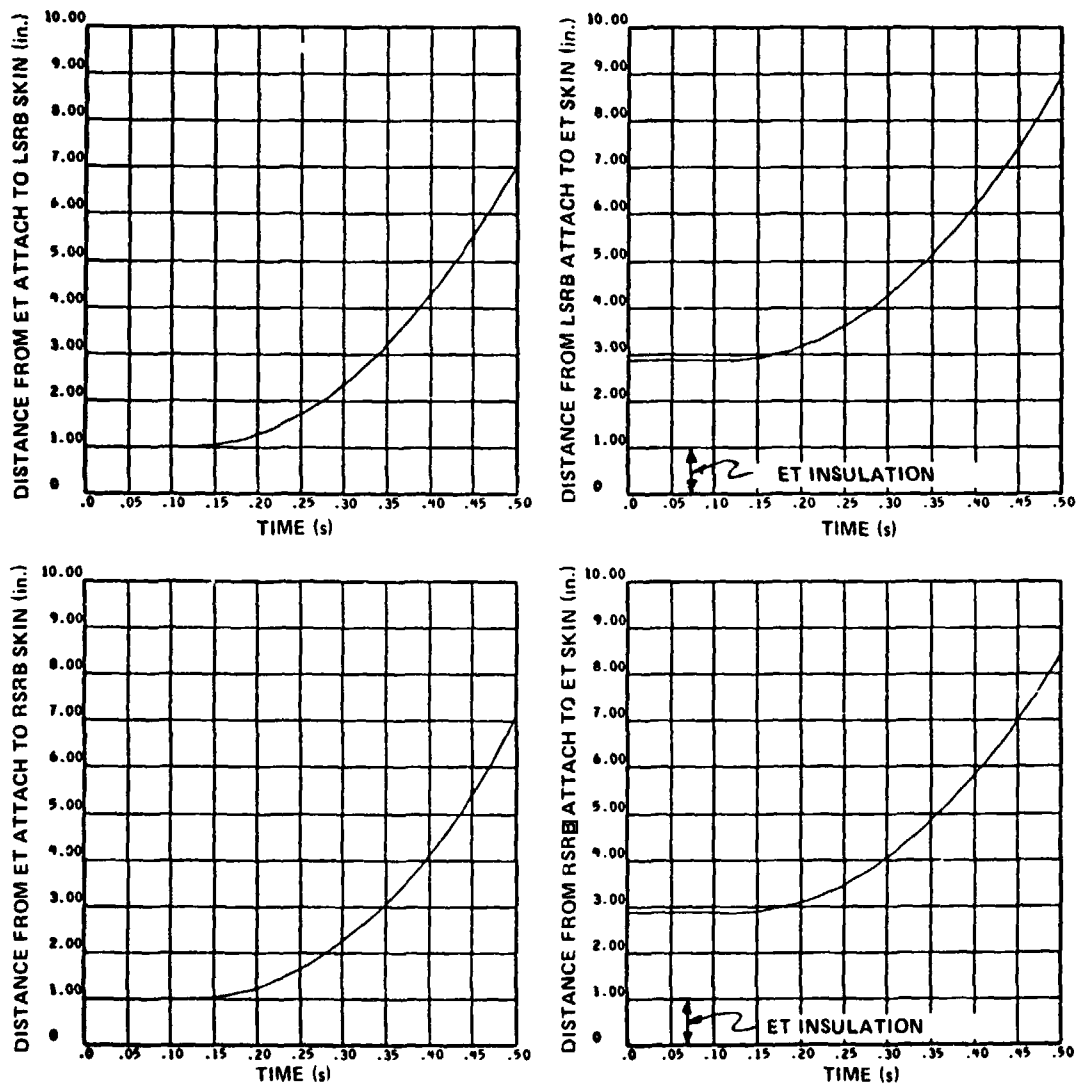
Figure 12. Separation clearances between SRB/ET forward attach structures
for worst case no-malfunction initial conditions with
a BSM failed on each SRB.
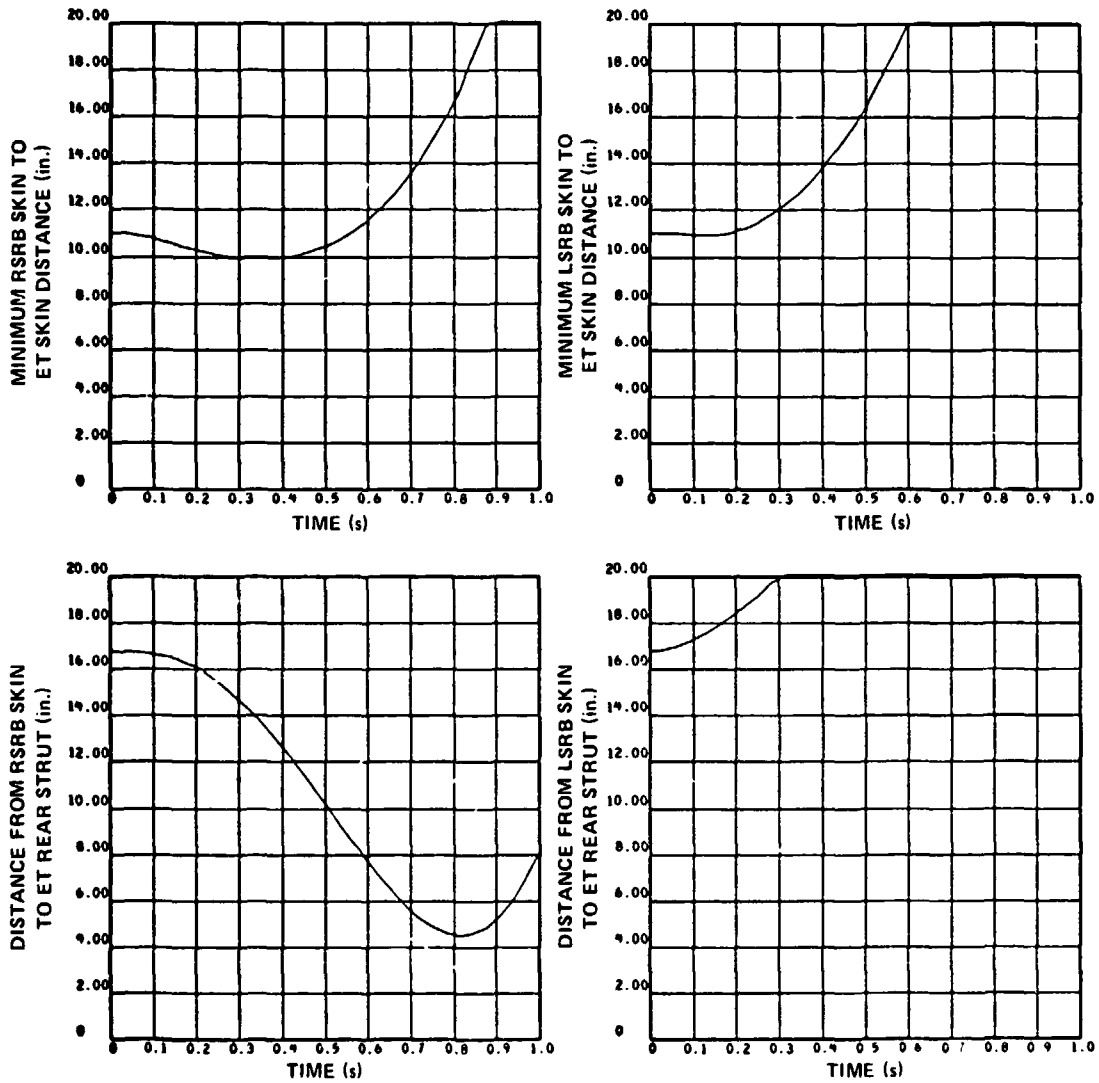
Figure 13. Separation clearances between SRB/ET skin-to-skin and
rear struts for worst case no-malfunction initial conditions
with a forward BSM failed on each SRB.
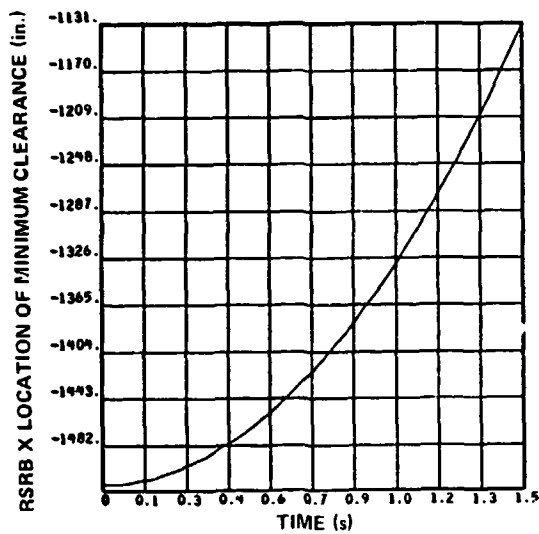
ET X LOCATION IS ALWAYS AFT END

(-2058 in.)
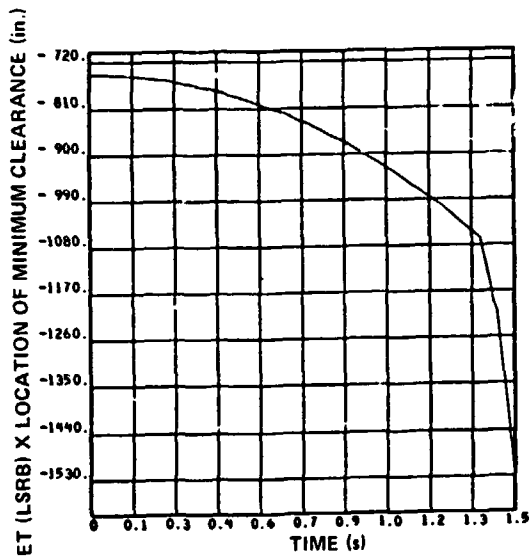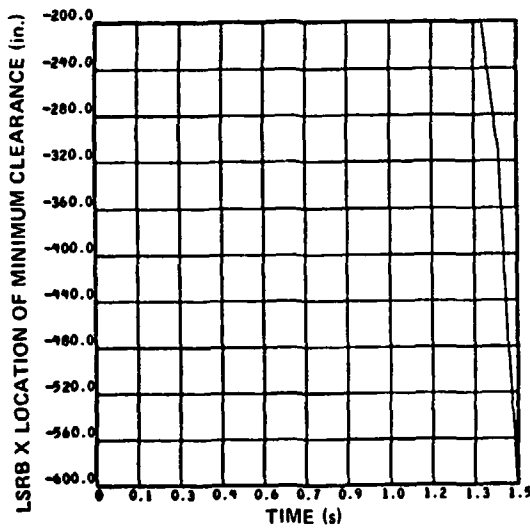
NOTE: SRB locations are SRB station numbers in the SRB
system and ET locations are ET station numbers in
the ET System (disregard the minus signs).

Figure 14. Axial location of minimum skin-to-skin clearance for worst
case no-malfunction initial conditions with a forward BSM
failed on each SRB.

29
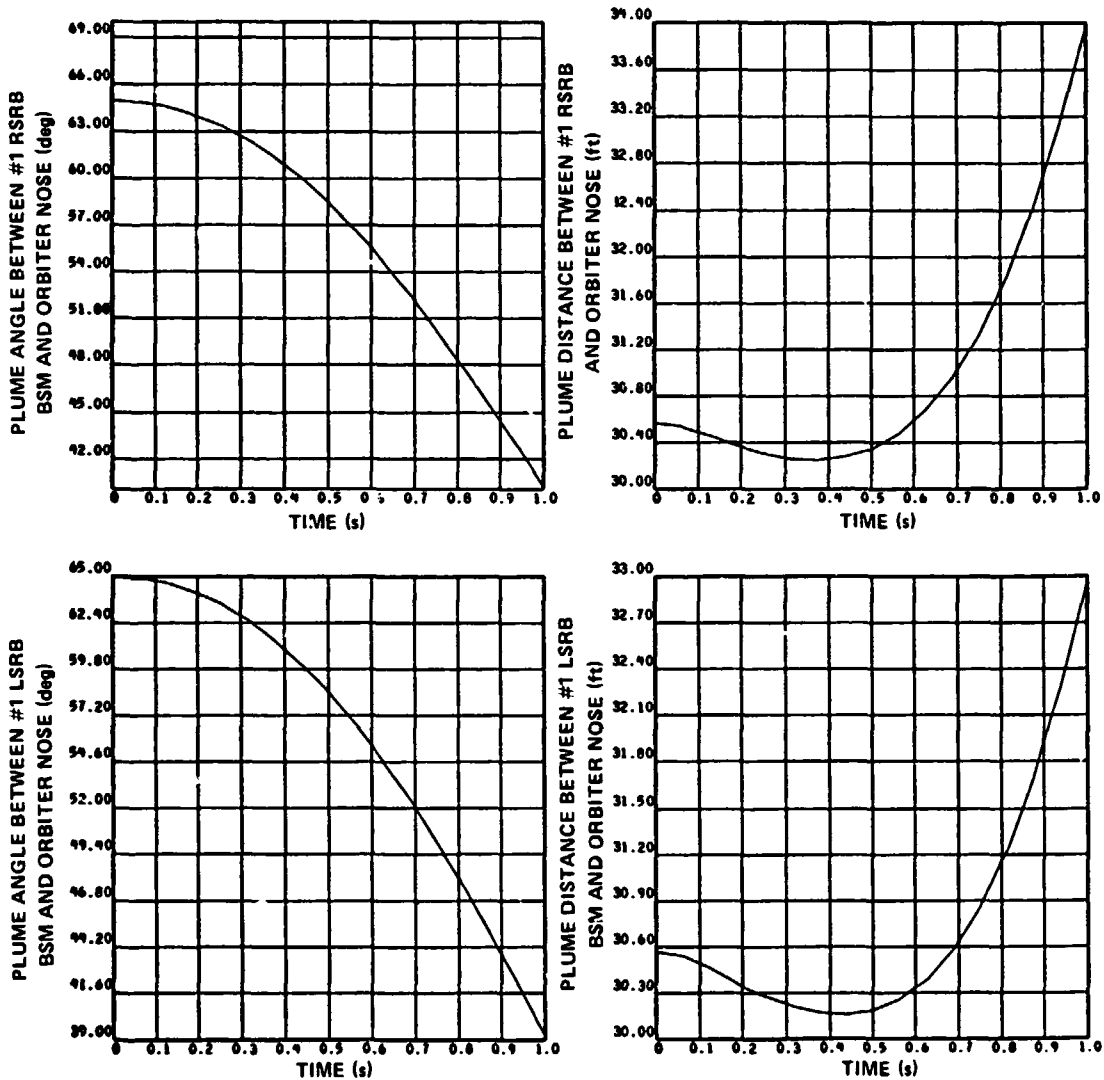
Figure 15. BSM #1 plume angle and distance to orbiter nose for worst
case no-malfunction initial conditions and a forward BSM
failed on each SRB.
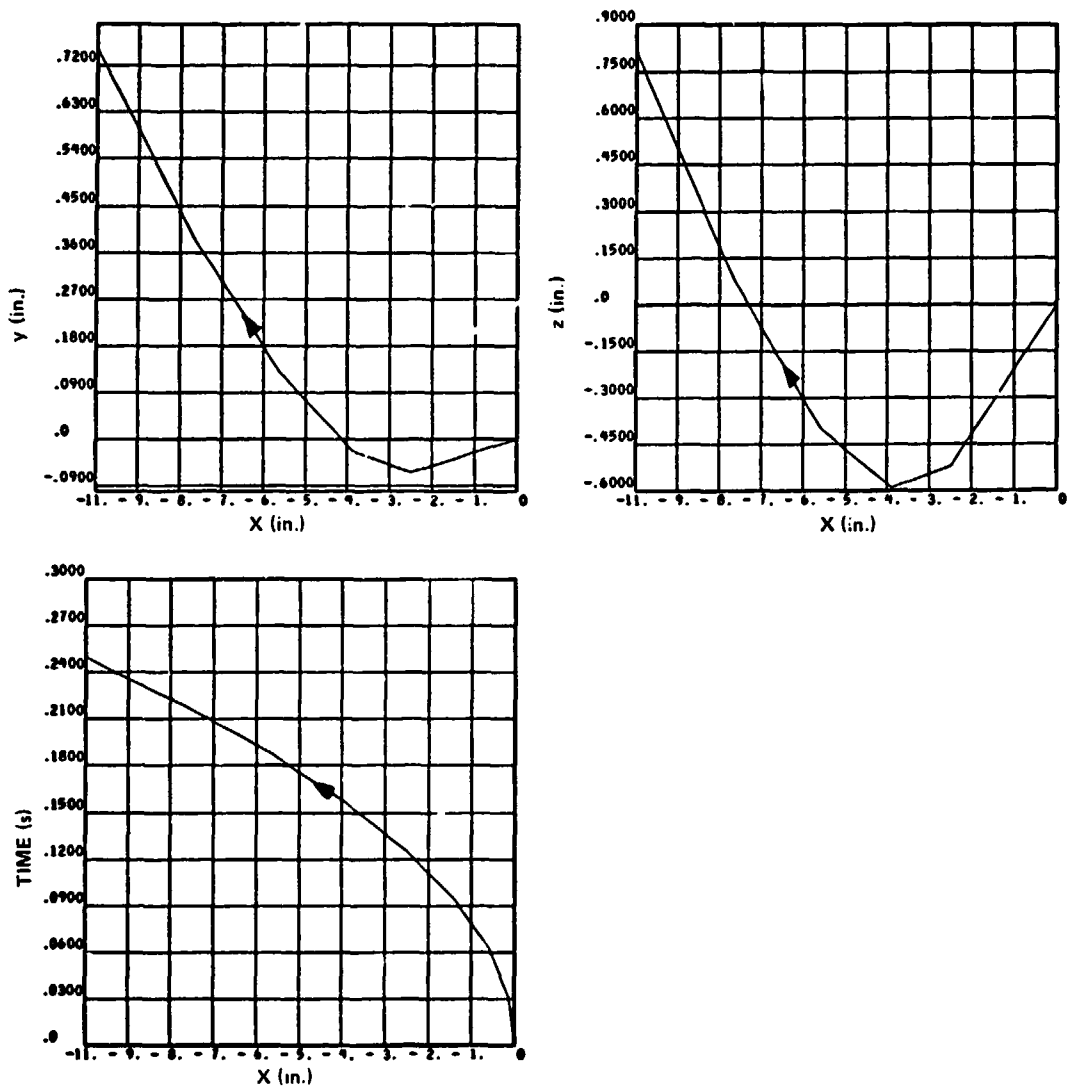
Figure 16. RSRB forward attach point motion with nominal initial conditions.
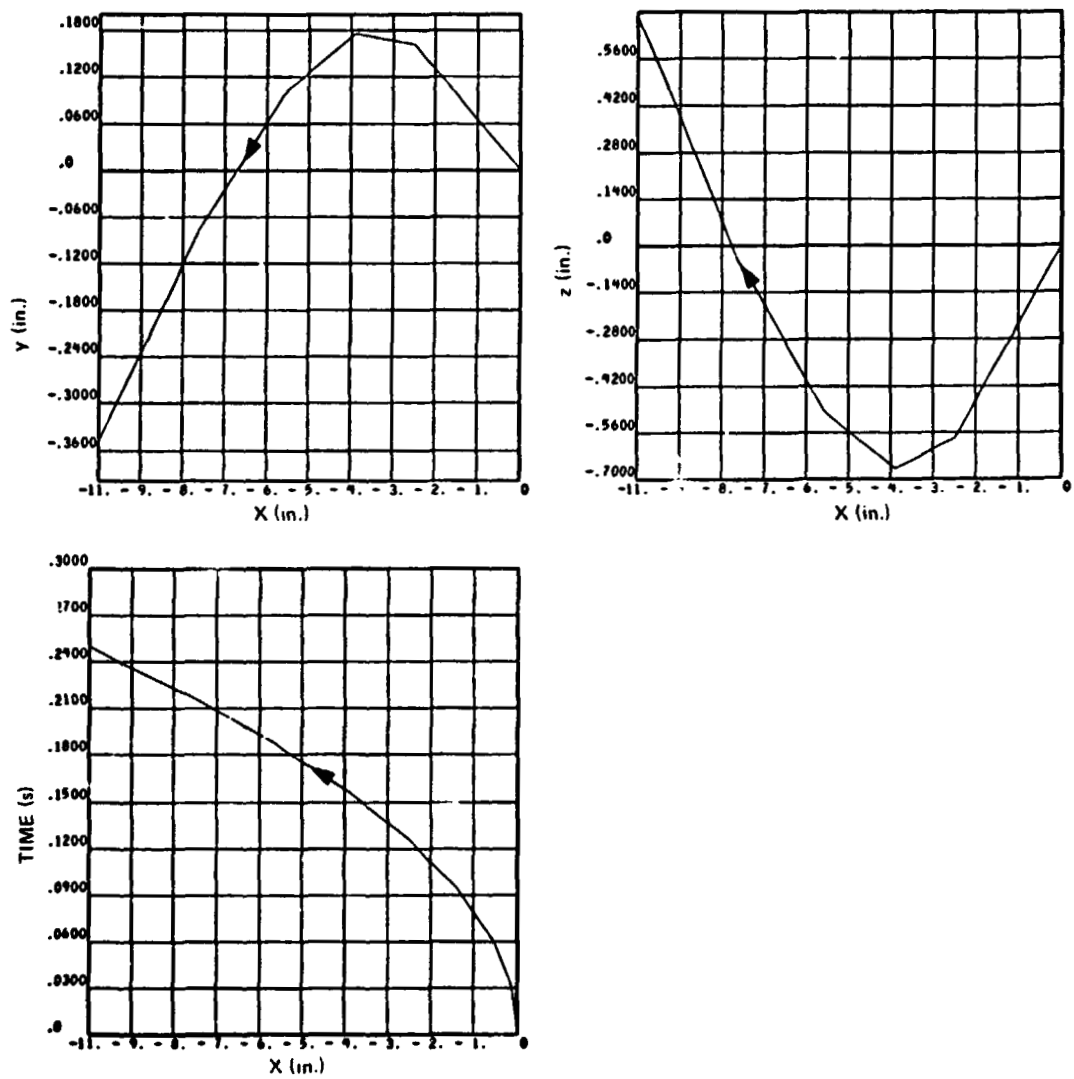
Figure 17. LSRB forward attach point motion with nominal initial conditions.
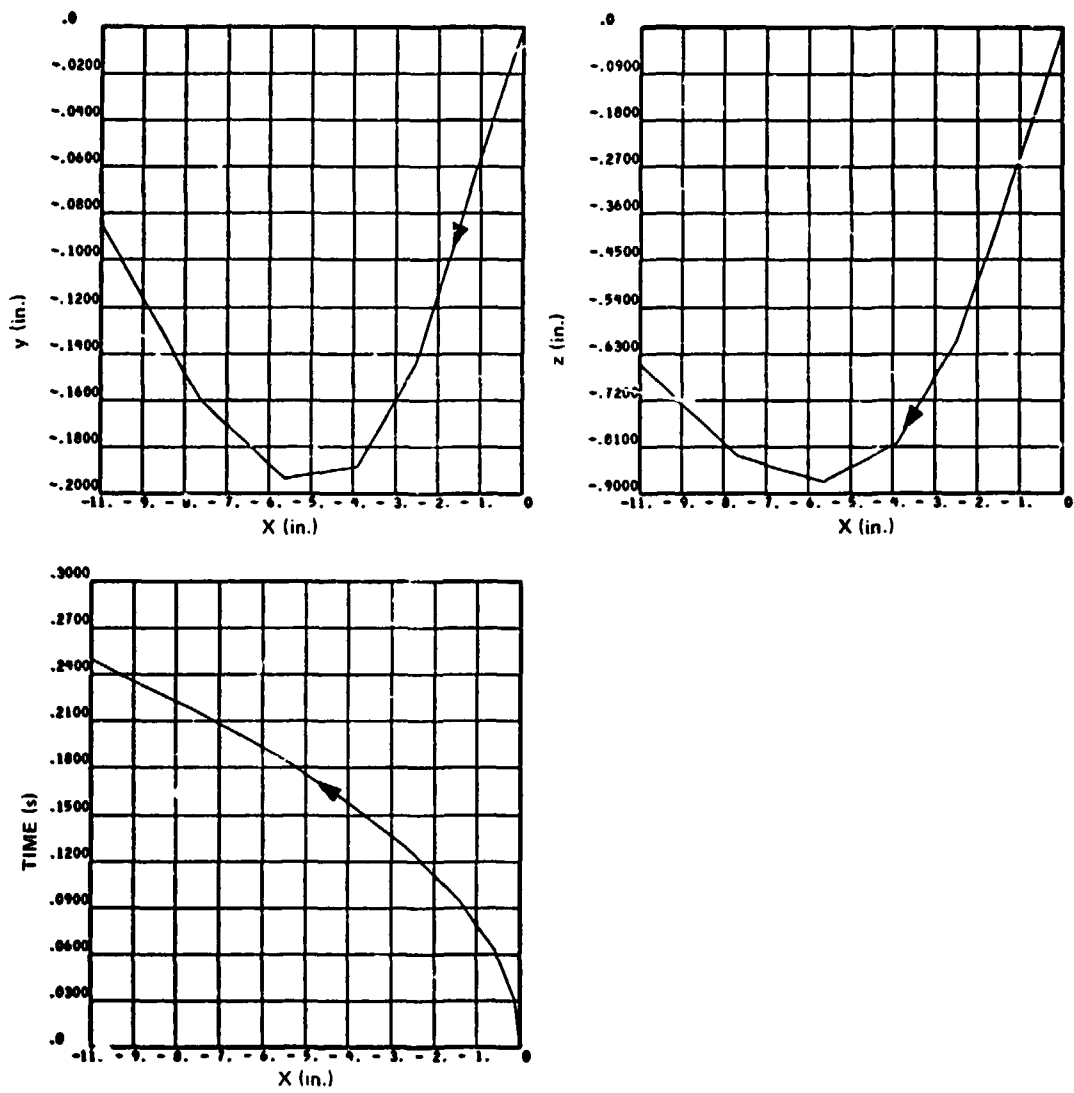
Figure 18. RSRB aft upper strut stub motion with nominal initial conditions.
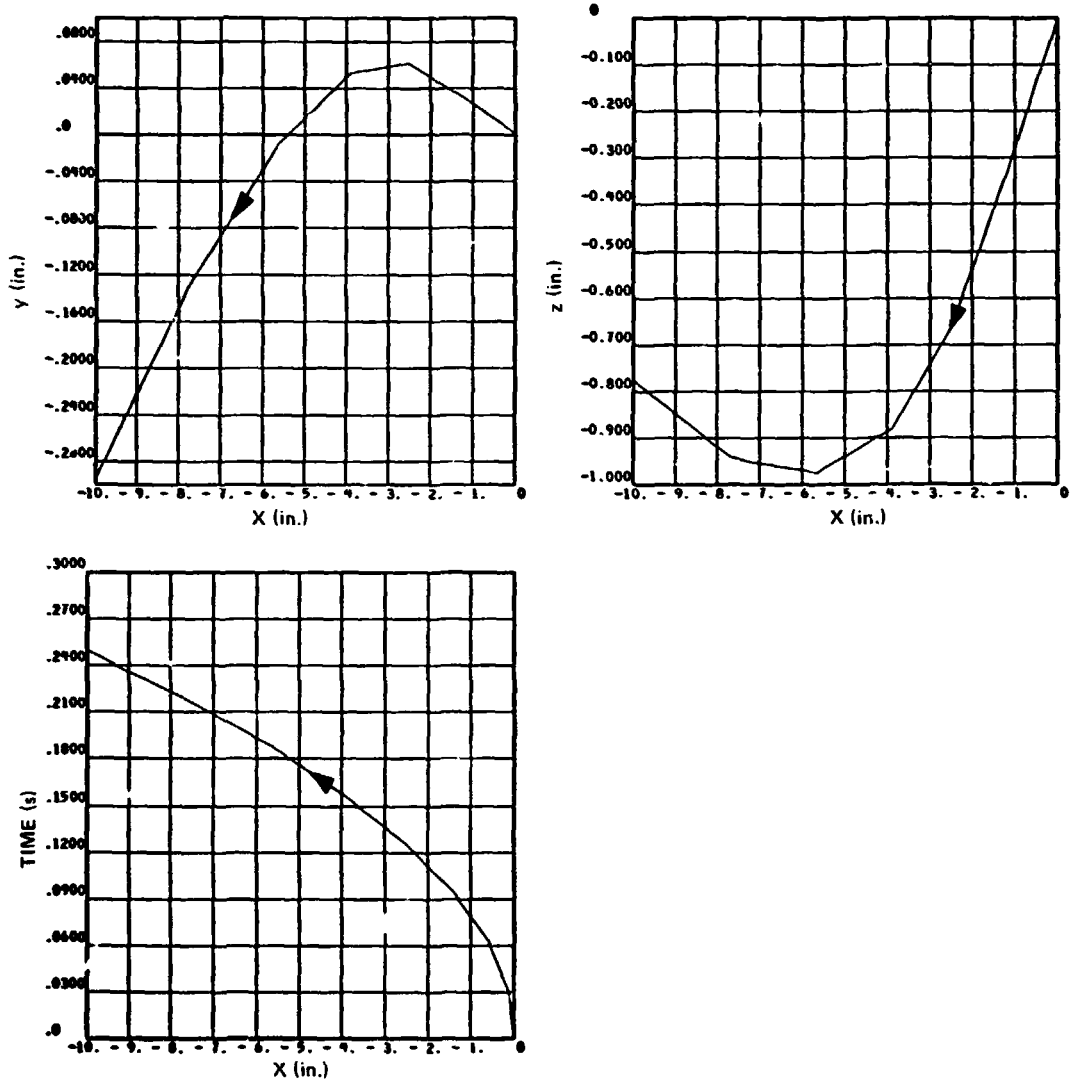
Figure 19. LSRB aft upper strut stub motion with nominal initial conditions.
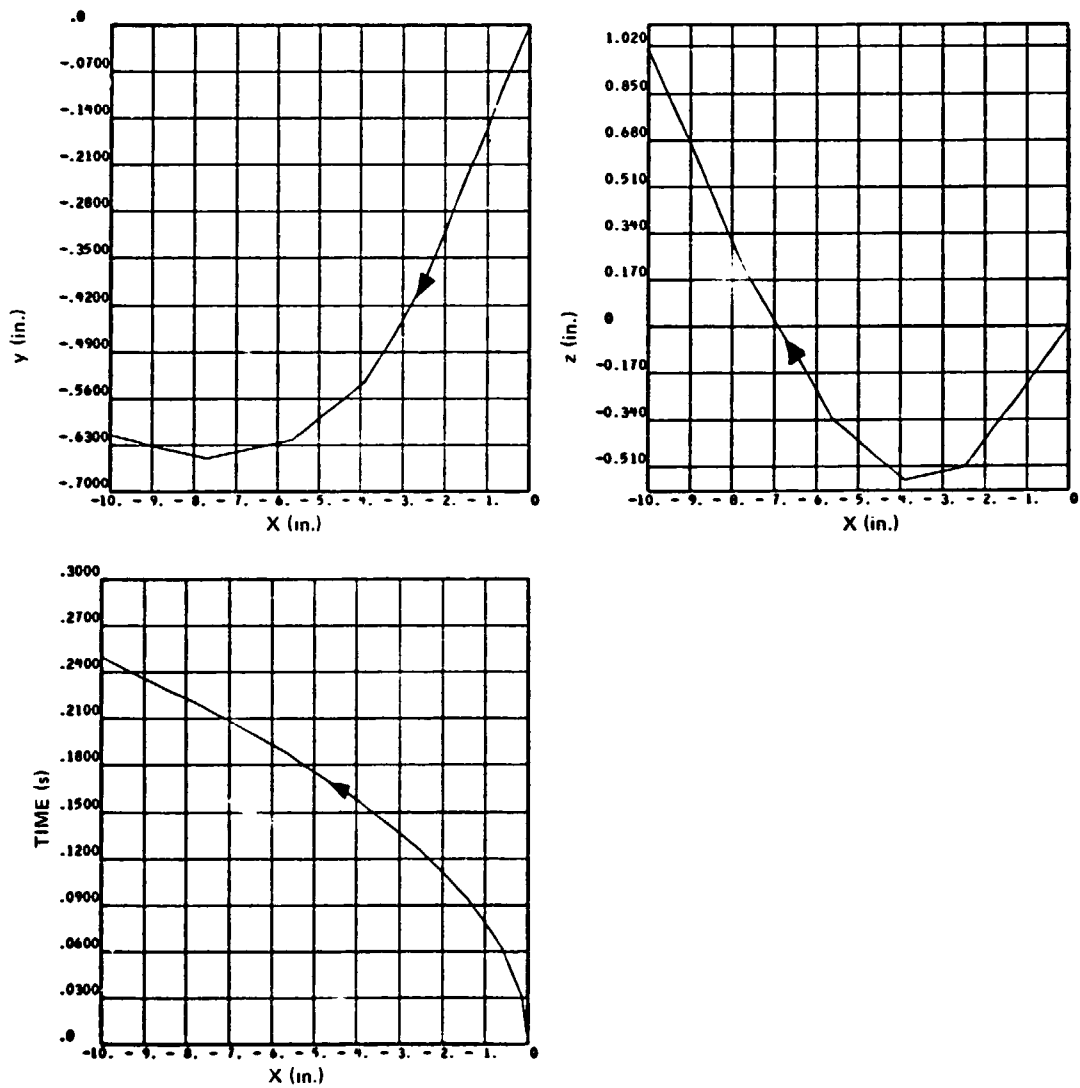
Figure 20. RSRB forward attach point motion with design initial conditions.
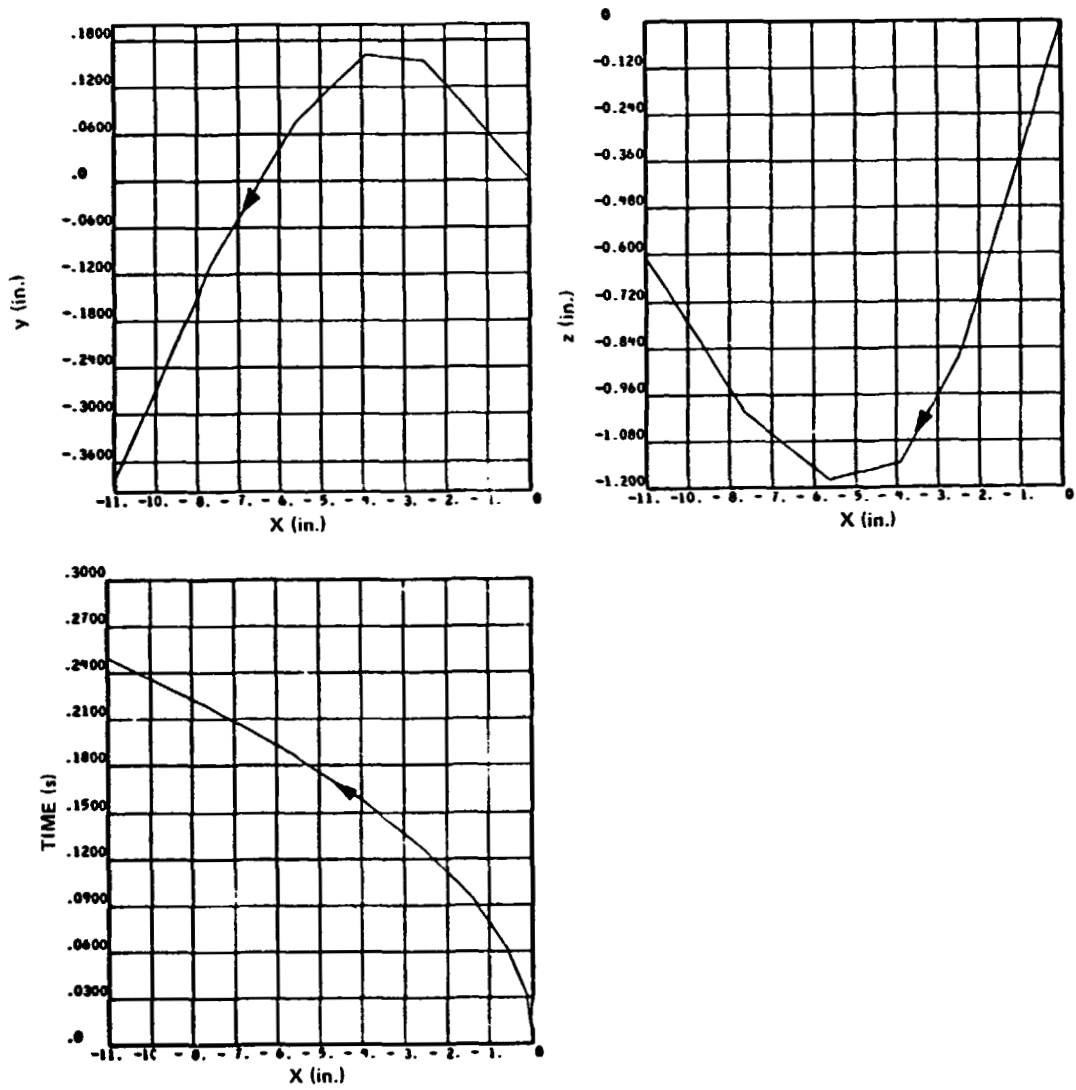
Figure 21. LSRB forward attach point motion for design initial conditions.
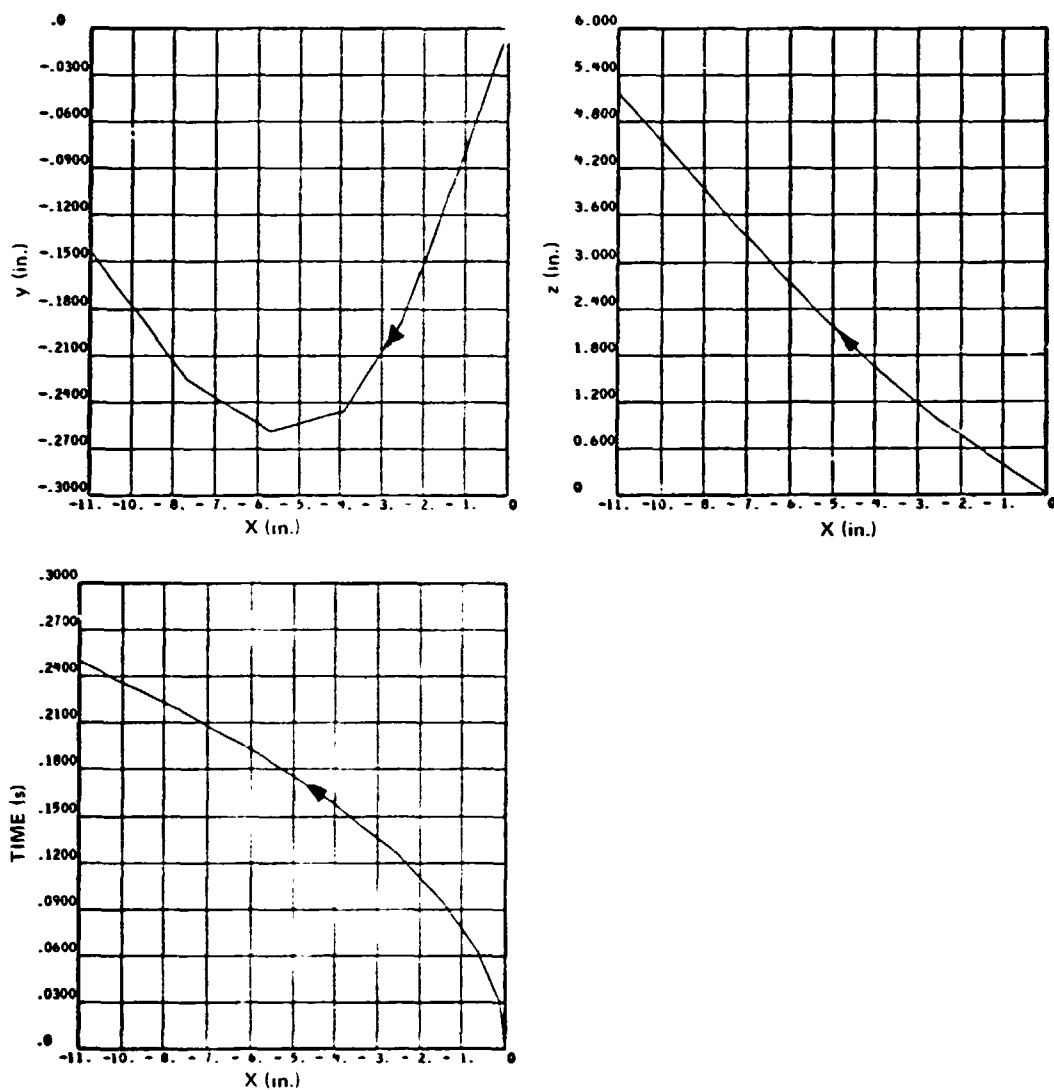
Figure 22. RSRB aft upper strut stub motion for design initial conditions.
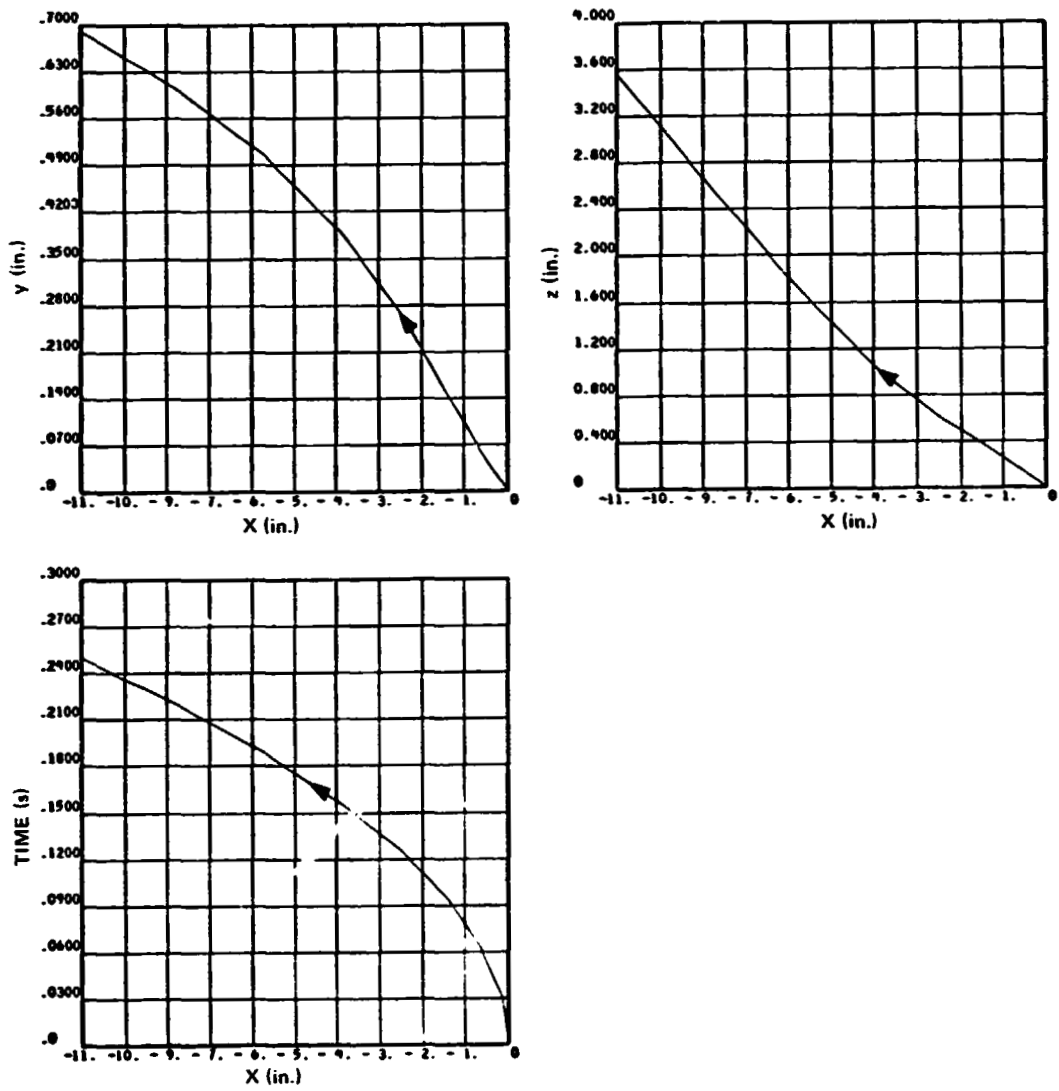
Figure 23.   LSRB aft upper strut stub motion for design initial conditions.

38

APPENDIX

COMPUTER PROGRAM AND AERODYNAMICS DESCRIPTION

This appendix describes the computer programs used to make the analyses and defines the aerodynamics which were used in these programs. The techniques of manipulating the aerodynamic data are delineated, and a critique of the aerodynamics is offered.

A. Computer Program Description

Two computer programs are used in the analysis of separation: (1) a Shuttle-mated ascent simulation is used to evaluate those factors which affect separation of the SRB and to examine techniques which will improve the initial conditions at separation; and (2) a three-body six-degree-of-freedom SRB separation simulation is used to evaluate the separation system capability and to determine factors which will improve separation.

1. Shuttle-Mated Ascent Computer Program

This program incorporates Configuration 5 mass properties and geometry, and the control system is the baseline (control mode 4) system. The program is oriented to control system studies but also accurately simulates the trajectory parameters so that the dynamic pressure at separation is of the proper value. The dynamic pressure is altered by winds and malfunctions; the separation is altered by the dynamic pressure. Therefore, it is important to have the proper trajectory simulation.

Special features are incorporated into this program to accurately develop the initial conditions at separation. The maximum thrust mismatch of the two SRB's shown in Figure A-1 was used in these analyses. It is one of the primary disturbances at separation. The SRB yaw cant caused by the internal pressure moving the nozzle out of the pressure chamber was simulated because it reduced the nozzle's gimbal capability. The cants on each of the SRB's are in opposite directions causing the forces from one SRB to oppose those of the other. The SRB has a snubber which supports the nozzle at water impact. The snubber is attached to the nozzle so that, when the

nozzle moves out of the pressure chamber during web action time, the snubber moves with it; thus the snubber does not restrict the nozzle gimbaling. However, during thrust decay, the snubber does restrict the nozzle gimbaling as shown in Figure A-2. Since it is undesirable for the snubber to contact the structure prior to water impact, a software-type vector limiter is included in the simulation.

Since the separation sequence is initiated when the SRB internal pressure is at or below 50 ± 15 psi, the program has the capability to start the separation sequence at a pressure of 50 ± 15 psi. At 0.8 seconds later, the SRB nozzles are commanded to null, the attitude reference is changed to momentarily zero the attitude error, and the control logic changes to second stage control logic. The ascent program does not drop the SRB's at staging time but continues as though the separation had been delayed. This feature allows the determination of time required to delay separation for those cases for which the design initial conditions are exceeded at separation.

2. Three-Body SRB Separation Simulation

This program simulates three bodies, each with six degrees of freedom. It calculates the aerodynamic forces on all three bodies which will be discussed in detail later. It can simulate all of the characteristics of a BSM. Each BSM is placed separately on the SRB's so that when simulating BSM-out the forces and moments will be correct. The impact routine determines if the bodies collide and gives the minimum clearances. However, the specific clearances to be checked have to be modeled in detail in this routine. At present, the impact routine gives the clearances between the following: (1) skin of the ET and SRB, (2) forward attach on the SRB and skin of the ET, (3) forward attach on the ET and skin of the SRB, and (4) aft bottom strut stub and SRB skin. The impact routine also gives the axial position where the minimum clearance exists and is given relative to the bodies centers of gravity (c.g.).

The Orbiter's insulation is fragile and cannot withstand impingement from a solid rocket motor. The solid particles penetrate the insulation and reduce its efficacy during reentry. Therefore, it is important to know if the BSM plumes impinge on the Orbiter. Consequently, the program plots the angles that the forward BSM plume centerlines make with the line from the BSM nozzle exit to

40

the Orbiter nose. The distance from the BSM nozzles to the Orbiter nose is also plotted.

The forward and aft close-in attach point motions are plotted versus axial movement and time. These data are used by designers of the interfaces. Additionally, the end conditions of the separation are used as the initial conditions for SRB recovery studies. After some coordination with recovery system analysts, a list of variables which would satisfy the recovery needs was developed as an output of the program.

B. Aerodynamics

The plume-on aerodynamics are used in the computer program during BSM thrust. The data are then switched to the "plume-off" aerodynamics for the remaining portion of the separation trajectory.

1. Plume-on Aerodynamics

The "plume-on" aerodynamics have two tables: OET data tables and right SRB (RSRB) data tables. The RSRB data tables can be used to generate the data for the left SRB (LSRB). All data are interpolated by constructing straight lines between the appropriate data points. When extrapolation is used, it is performed by using the slope formed by the last two data points used for interpolation.

a. OET Aerodynamics

The OET data are looked up versus the axial displacement (X) and the radial displacement (R) of the nose of the individual SRB's (see Figure A-3). In some of the coefficients, the X-lookup parameter has been omitted, and the coefficient is looked up for R only. A definition of the coefficients is shown in Figure A-4. In the following equations, the terms inside the parentheses are the parameters used to look up the coefficients. The axial force coefficient (C_A) is a pure table lookup, that is

$$C_{A_{OET}} = C_{A_{OET}} \left(\frac{R_{LSRB} + R_{RSRB}}{2} \right),$$

where the lookup parameter is the average radial (R) displacement of the two SRB's. The normal force coefficient (C_N) is calculated by the following

$$C_{N_{\alpha_{OET}}} = \left. C_{N_{\alpha_{OET}}}(R_{RSRB}) + C_{N_{\alpha_{OET}}}(R_{LSRB}) \right/ 2,$$

$$C_{N_{O_{OET}}} = C_{N_{O_{OET}}}\left(\frac{R_{LSRB} + R_{RSRB}}{2}, \frac{X_{LSRB} + X_{RSRB}}{2}\right)$$

$$C_{N_{OET}} = C_{N_{O_{OET}}} + C_{N_{\alpha_{OET}}}\alpha_{OET} + C_{N_{\alpha_{RSRB}}}(R_{RSRB}, X_{RSRB})\alpha_{RSRB}$$

$$+ C_{N_{\alpha_{LSRB}}}(R_{LSRB}, X_{LSRB})\alpha_{LSRB}.$$

A blend of the average of the SRB positions with the positions of the LSRB and RSRB is used to look up and calculate the OET normal force in order to accurately simulate the proximity effects of the SRB's on the OET. The pitching moment coefficient is calculated by the same procedure, that is,

$$C_{M_{\alpha_{OET}}} = \left[C_{M_{\alpha_{OET}}}(R_{SRB}) + C_{M_{\alpha_{OET}}}(R_{LSRB})\right]\Big/2$$

$$C_{M_{O_{OET}}} = C_{M_O}\left(\frac{R_{LSRB} + R_{RSRB}}{2}, \frac{X_{LSRB} + X_{RSRB}}{2}\right)$$

$$C_{M_{OET}} = C_{M_{O_{OET}}} + C_{M_{\alpha_{OET}}}\alpha_{OET} + C_{M_{\alpha_{RSRB}}}(R_{RSRB}, X_{RSRB})\alpha_{RSRB}$$

$$+ C_{M_{\alpha_{LSRB}}}(R_{LSRB}, X_{LSRB})\alpha_{LSRB}.$$

The lateral directional coefficients are calculated using the same method. The side force (C_Y), yawing moment (C_n), and rolling moment (C_ℓ) coefficients are obtained as follows:

$$C_{Y_{OET}} = \left\{ \left[C_{Y_{\beta_{OET}}}(R_{RSRB}) + C_{Y_{\beta_{OET}}}(R_{LSRB}) \right] \Big/ 2 \right\} \beta_{OET}$$

$$C_{n_{OET}} = \left\{ \left[C_{n_{\beta_{OET}}}(R_{RSRB}) + C_{n_{\beta_{OET}}}(R_{LSRB}) \right] \Big/ 2 \right\} \beta_{OET}$$

$$C_{\ell_{OET}} = \left\{ \left[C_{\ell_{\beta_{OET}}}(R_{RSRB}) + C_{\ell_{\beta_{OET}}}(R_{LSRB}) \right] \Big/ 2 \right\} \beta_{OET} .$$

A critique of these data is provided so that the proper qualification of the results of this study can be drawn. The critique is enumerated below:

(1)   The coefficients are a function of insufficient parameters. They should vary versus the three displacement parameters, the relative incident angles of the SRB's to the OET, and the angle of attack and side slip of the OET.

(2)   Only RSRB data were taken in the wind tunnel so that the effects of the LSRB in the presence of the OET and RSRB are not known, but the effects of the LSRB on the OET can be reasonably assumed to be similar to those of the RSRB.

(3)   Since the proximity effects are not separated from the total aerodynamic effects, it is not possible to determine the correct coefficients for the effects on the OET due to the LSRB. That is, in some cases, the proximity effects are additive, but, if the coefficients are added, the isolated effect will be twice the proper value. Also, the side force proximity effect tends to cancel out, but, if the coefficients are subtracted, the isolated effect will be set to zero.

(4)   The SSME plumes tend to destabilize the OET. These plumes were not simulated in the wind tunnel test and, consequently, the OET would appear to be more stable than it really is.

b.   RSRB Aerodynamics

These coefficients are lookup versus the same parameters as those for the OET (see Figure 8). The axial force coefficient (C_A) is obtained by

$$C_{A_{RSRB}} = C_{A_{RSRB}}(R_{RSRB}) \quad ,$$

which is simply a table lookup for the radial displacement. The normal force (C_N) and pitching moment (C_M) coefficients are obtained by

$$C_{N_{RSRB}} = C_{N_{O_{RSRB}}}(R_{RSRB}, X_{RSRB}) + C_{N_{\alpha_{OET}}}(R_{RSRB}) \alpha_{OET}$$

$$+ C_{N_{\alpha_{RSRB}}}(R_{RSRB}, X_{RSRB}) \alpha_{RSRB}$$

$$C_{M_{RSRB}} = C_{M_{O_{RSRB}}}(R_{RSRB}, X_{RSRB}) + C_{M_{\alpha_{OET}}}(R_{RSRB}) \alpha_{OET}$$

$$+ C_{M_{\alpha_{RSRB}}}(R_{RSRB}, X_{RSRB}) \alpha_{RSRB}.$$

The side force (C_Y) and the yawing moment (C_n) coefficients are calculated as follows:

44

$$C_{Y_{RSRB}} = C_{Y_{O_{RSRB}}}(R_{RSRB}, X_{RSRB}) + C_{Y_{\beta_{OET}}}(R_{RSRB})\,\beta_{OET}$$

$$+ \left[C_{Y_{\beta_{RSRB}}}(R_{RSRB}) + C_{Y_{\beta_{RSRB}\beta_{OET}}}(R_{RSRB})\,\beta_{OET} \right]\beta_{RSRB}$$

$$C_{n_{RSRB}} = C_{n_{O_{RSRB}}}(R_{RSRB}, X_{RSRB}) + C_{n_{\beta_{OET}}}(R_{RSRB})\,\beta_{OET}$$

$$+ \left[C_{n_{\beta_{RSRB}}}(R_{RSRB}) + C_{n_{\beta_{RSRB}\beta_{OET}}}(R_{RSRB})\,\beta_{OET} \right]\beta_{RSRB}.$$

The roll moment was assumed to be small so that the coefficient (C_ℓ) was set to zero. The following is a critique of these data:

(1)   These coefficients are a function of insufficient parameters. They should vary versus the three displacement parameters, the relative incident angles of the S^nB to OET, and the angle of attack and side slip oɪ the OET.

(2)   Since the RSRB data were measured in the wind tunnel, the data for the RSRB should be fairly representative.

(3)   The roll moment will not be zero, so there is some error in setting the coefficient to zero.

c.   LSRB Aerodynamics

The LSRB aerodynamics are derived from the RSRB data since there was no LSRB in the wind tunnel test. The equations for the longitudinal coefficients of the LSRB are the same as for RSRB except, of course, the look ᴏ parameters and α are for the LSRB. Since no roll moment data exist for the RSRB, the LSRB must also be assumed to be zero. The side force and yawing moment coefficients

change some of the signs in the equations to account for the LSRB being on the opposite side of the OET from the RSRB (since only RSRB data exists), that is

$$C_{Y_{LSRB}} = -C_{Y_{O_{LSRB}}}(R_{LSRB}, X_{LSRB}) + C_{Y_{\beta_{OET}}}(R_{LSRB})\,\beta_{OET}$$

$$+ \left[C_{Y_{\beta_{LSRB}}}(R_{LSRB}) - C_{Y_{\beta_{LSRB}\,\beta_{OET}}}(R_{LSRB})\,\beta_{OET} \right]\beta_{LSRB}$$

$$C_{n_{LSRB}} = -C_{n_{O_{LSRB}}}(R_{LSRB}, X_{LSRB}) + C_{n_{\beta_{OET}}}(R_{LSRB})\,\beta_{OET}$$

$$+ \left[C_{n_{\beta_{LSRB}}}(R_{LSRB}) - C_{n_{\beta_{LSRB}\,\beta_{OET}}}(R_{LSRB})\,\beta_{OET} \right]\beta_{LSRB}.$$

The intercept value in these two equations should represent pure proximity effects since the isolated C_Y is normally zero for $\beta_{LSRB} = 0$. Consequently, the proximity effects should be opposite signs for the LSRB versus the RSRB. The second coefficient $(C_{i_{\beta_{OET}}})$ of the two equations does not change sign because, assuming that the RSRB is on the windward side, then LSRB is on the leeward side. Therefore, the sign of β_{OET} must be changed to make the RSRB slope appear to be on the leeward side. Since the results represent a RSRB with a $-\beta_{OET}$, the sign of the results must be changed to represent a LSRB with a $+\beta_{OET}$, which is the same as no sign change. No change in sign is necessary for the third coefficient $(C_{i_{\beta_{SRB}}})$ since the term represents primarily isolated effects. The remaining coefficient $(C_{i_{\beta_{SRB}\,\beta_{OET}}})$ changes sign because the rate of change of $C_{i_{\beta_{SRB}}}$ for the LSRB with respect

to β_{OET} is in the opposite direction from the RSRB. The critique of the LSRB plume-on aerodynamics is as follows:

(1)   These coefficients are a function of insufficient parameters. They should vary versus the three displacement parameters, the relative incident angles of the SRB to OET and the angle of attack and side slip of the OET.

(2)   The roll moment will not be zero, so there is some error in setting the coefficient to zero.

(3)   The longitudinal coefficients should be representative since effects should be the same on the LSRB and RSRB.

2.   Plume-off Aerodynamics

The plume-off aerodynamics have eight tables: two isolated aerodynamic tables (SRB and OET), two proximity intercept tables (RSRB and OET), and four proximity slope tables (slopes for total and isolated coefficients for both RSRB and OET). In the proximity slope calculations, the isolated slope data are subtracted from the total coefficients so that the results will represent pure proximity effects. Like the plume-on aerodynamics, all interpolations and extrapolations are performed linearly.

a.   OET Aerodynamics

The plume-off OET aerodynamics are comprised of three parts: proximity intercept data, proximity slope data and isolated data. The proximity intercept data are stored in tables and looked up for the following five variables: $\alpha = \alpha_{SRB} - \alpha_{OET}$, $\beta = \beta_{SRB} - \beta_{OET}$, X, Y and Z where the X, Y and Z are SRB nose displacements from the initial position. Since the intercept data are for $\alpha_{OET} = 0$ and $\beta_{OET} = 0$, the proximity slope data are used to extrapolate these data for the OET at α and β. These slope data are only a function of the Z-displacement. The isolated aerodynamics are combined with the proximity data as follows:

$$C = C_{PROX_{\substack{\alpha=0 \\ \beta=0}}}(\Delta\alpha, \Delta\beta, X, Y, Z) + \left[C_{T_{\alpha_{OET}}}(Z) - C_{ISOL\alpha_{OET}} \right]_{PROX}{}^{\alpha_{OET}}$$

$$+ \left[C_{T_{\beta_{OET}}}(Z) - C_{ISOL\,\beta_{OET}} \right]_{PROX}{}^{\beta}\,OET + C_{ISOL_{\substack{\alpha=0 \\ \beta=0}}}$$

$$+ C_{ISOL_{\alpha_{OET}}}(SGN\left[\alpha_{OET}\right])\,\alpha_{OET} + \left\{ C_{ISOL\,\beta_{OET}}(SGN\left[\beta_{OET}\right]) \right.$$

$$+ \left. C_{ISOL\,\beta_{OET}\,\alpha_{OET}}(SGN\left[\alpha_{OET}\right], SGN\left[\beta_{OET}\right])\,\alpha_{OET} \right\}\,\beta_{OET} \quad,$$

where

$$C_{PROX_{\substack{\alpha=0 \\ \beta=0}}} = \left[C_{PROX_{\substack{\alpha=0 \\ \beta=0}}}(\Delta\alpha_{RSRB}, \Delta\beta_{RSRB}, X_{RSRB}, Y_{RSRB}, Z_{RSRB}) \right.$$

$$+ C_{PROX_{\substack{\alpha=0 \\ \beta=0}}}(\Delta\alpha_{LSRB}, \Delta\beta_{LSRB}, X_{LSRB}, Y_{LSRB}, Z_{LSRB})$$

$$+ 2C_{PROX_{\substack{\alpha=0 \\ \beta=0}}}\left(\frac{\Delta\alpha_{RSRB} + \Delta\alpha_{LSRB}}{2}, \frac{\Delta\beta_{RSRB} + \Delta\beta_{LSRB}}{2}, \right.$$

$$\left. \left. \frac{X_{RSRB} + X_{LSRB}}{2}, \frac{Y_{RSRB} + Y_{LSRB}}{2}, \frac{Z_{RSRB} + Z_{LSRB}}{2}\right) \right] \Big/ 4$$

$$C_{T_{\alpha_{OET}}} = \left[C_{T_{\alpha_{OET}}}(Z_{RSRB}) + C_{T_{\alpha_{OET}}}(Z_{LSRB}) + 2\, C_{T_{\alpha_{OET}}}\left(\frac{Z_{RSRB}+Z_{LSRB}}{2}\right) \right] \Big/ 4.$$

The coefficients are stored in the OET aerodynamic data array as though the SRB's are symmetrically located about the OET. Consequently, for the intercept $(C_{PROX_{\alpha=0}^{\beta=0}})$, C_Y, C_n, and C_ℓ are all zero and only C_A, C_N and C_M are looked up for the five variables. However, an extrapolation is made for all of the coefficients. The coefficients $C_{T_{\alpha_{OET}}}$ and $C_{T_{\beta_{OET}}}$ are the total coefficients which are measured on the OET in the presence of the SRB's. The isolated coefficients, $C_{ISOL_{\alpha_{OET}}}$ and $C_{ISOL_{\beta_{OET}}}$, are subtracted from the total coefficient to reduce the data to pure proximity data. The intercept coefficient $(C_{PROX_{\alpha=0}^{\beta=0}})$ represents pure proximity data. The data are used in the pure proximity form so that the right-hand data can be used for the left-hand data by the appropriate sign changes. $SGN[\alpha_{OET}]$ and $SGN[\beta_{OET}]$ are used to indicate that the coefficient is looked up for the sign on α and β. The sign of β causes some of the coefficients to change sign but does not affect the magnitude, while the sign of α causes some of the coefficients to change magnitude but does not affect the sign. The critique of these data is as follows:

(1)   The data assume symmetrically located SRB's.
        In many of the separations, the SRB's are not
        symmetrical. Attempts were made to make up
        for this lack of symmetry (as shown in the latter
        two equations) but this was only an approximation.

(2)   The proximity data were linearly extrapolated for
        α and β, and it is highly improbable that the
        proximity data are linear.

(3) The SSME plumes were not simulated in the wind tunnel tests. These plumes tend to destabilize the OET; consequently, the OET appears more stable than it really is.

b. <u>SRB Aerodynamics</u>

The plume-off data for the SRB's are similar to the OET. The equation for the RSRB coefficient is

$$C = C_{PROX_{\substack{\alpha=0 \\ \beta=0}}} (\Delta\alpha, \Delta\beta, X, Y, Z)_{RSRB}$$

$$+ \left[C_{T_{RSRB_{\alpha_{OET}}}} (Z) - C_{ISOL_{RSRB_{\alpha_{OET}}}} \right]_{PROX} \alpha_{OET}$$

$$+ \left[C_{T_{RSRB_{\beta_{OET}}}} (Z) - C_{ISOL_{RSRB_{\beta_{OET}}}} \right]_{PROX} \beta_{OET}$$

$$+ C_{ISOL_{RSRB_{\substack{\alpha=0 \\ \beta=0}}}} + C_{ISOL_{\alpha_{RSRB}}} \alpha_{RSRB} + C_{ISOL_{\beta_{RSRB}}} \beta_{RSRB}.$$

The proximity intercept coefficient ($C_{PROX_{\substack{\alpha=0 \\ \beta=0}}}$), which is looked up for the five variables, exists for the following five coefficient calculations: C_N, C_M, C_Y, C_n. Also, only these same coefficients are extrapolated for α_{OET} and β_{OET} at some value other than zero. It is assumed that for proximity effects C_A and C_ℓ are zero for the SRB's. The isolated data are not looked up but are single-valued, and data exist for only the same coefficients; that is, C_N, C_M, C_Y and C_n. For the isolated data, C_ℓ is assumed zero, but the axial force coefficient is calculated as follows:

50

$$C_A = C_{A_O} + C_{A_{\alpha_T}} \, \alpha_T \, ,$$

where

$$\alpha_T = \sqrt{\alpha^2 + \beta^2} \, .$$

The LSRB equations are the same as those for the RSRB with the exceptions noted in this paragraph. Only RSRB data exist. For the proximity effects, certain manipulations are required to make RSRB data appropriate for the LSRB. The isolated data require no alterations. The proximity intercept data $(C_{PROX_{\substack{\alpha=0 \\ \beta=0}}})$ are looked up for the five LSRB parameters, but the sign of the LSRB's $\Delta\beta$ must be changed because the definition of $\Delta\beta$ causes the sign of $\Delta\beta$ to be different for a symmetric case. After the data have been looked up for $(C_{PROX_{\substack{\alpha=0 \\ \beta=0}}})$, the sign of the C_Y and C_n coefficients must be changed because, for the proximity effects, the lateral-directional data are in opposite directions for the LSRB. The sign of β_{OET} must be changed for all of the coefficients of the LSRB in the proximity extrapolation equations so that the RSRB data will be appropriate for the LSRB.

The critique of the SRB plume-off aerodynamics is given below:

(1)   The proximity data were linearly extrapolated for α and β and it is highly improbable that these data are linear.

(2)   The roll moment and axial force on the SRB's due to proximity effects will be small but probably not zero as was assumed herein.

(3)   The roll moment was also assumed zero for the isolated data. There should be some roll moment on the SRB's.
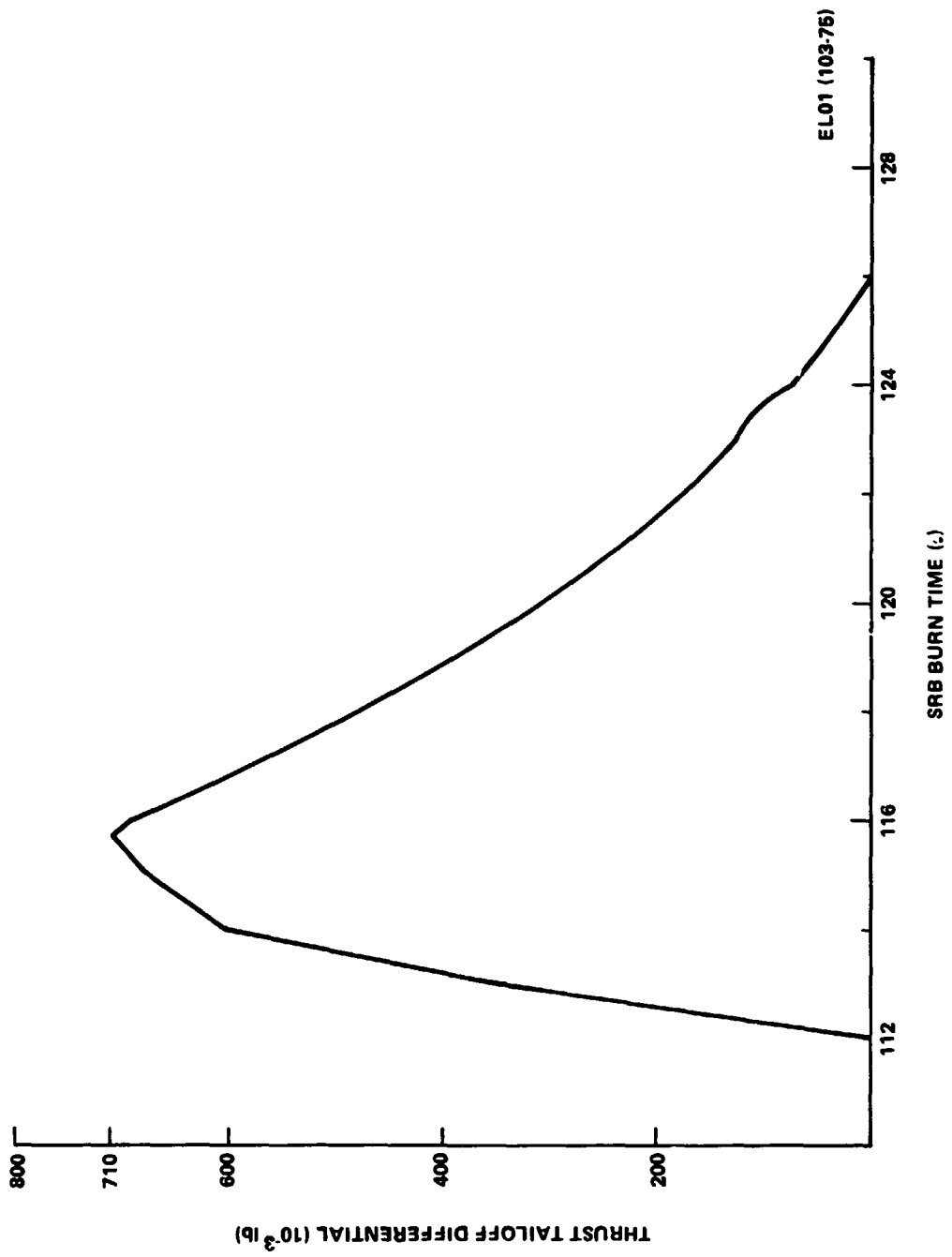
Figure A-1. SRB thrust mismatch during thrust tailoff.
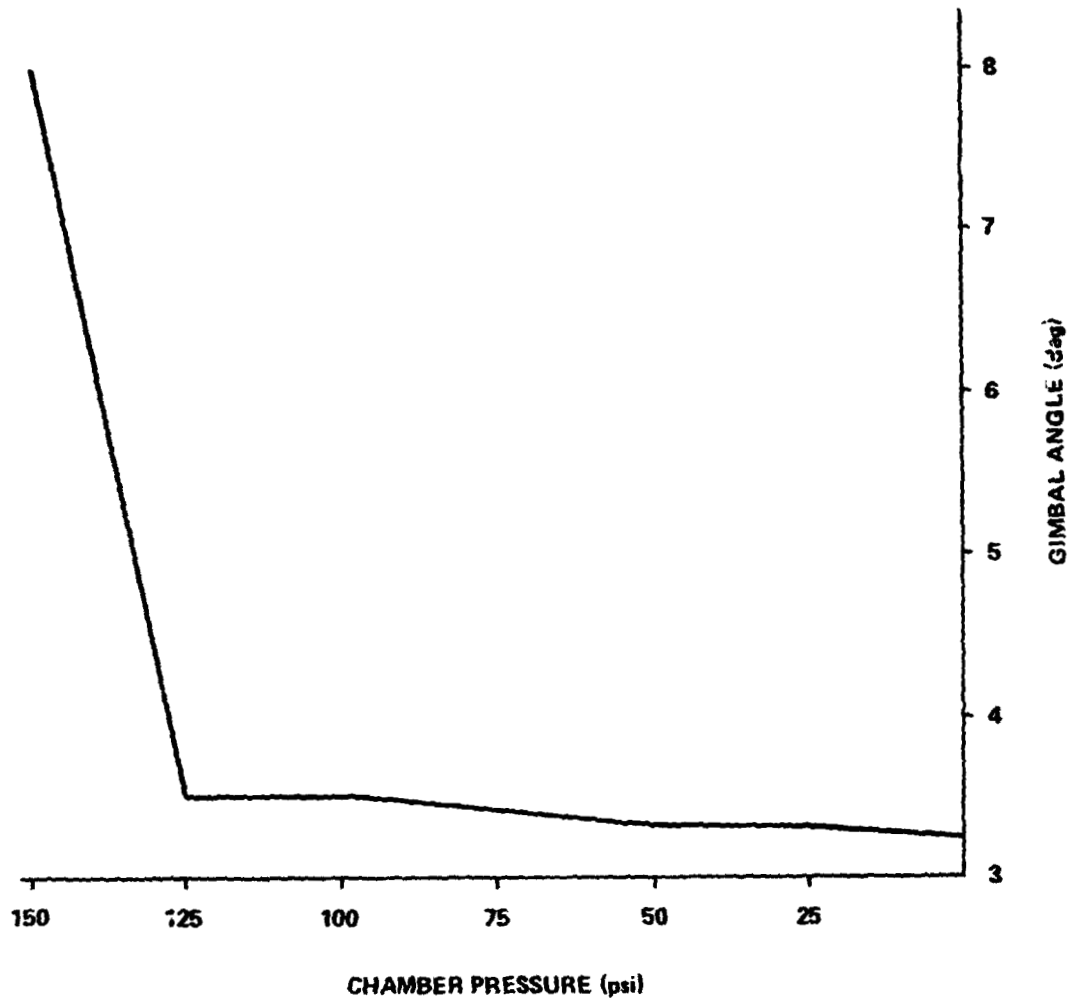
Figure A-2. SRB gimbal limit to prevent snubber contact.
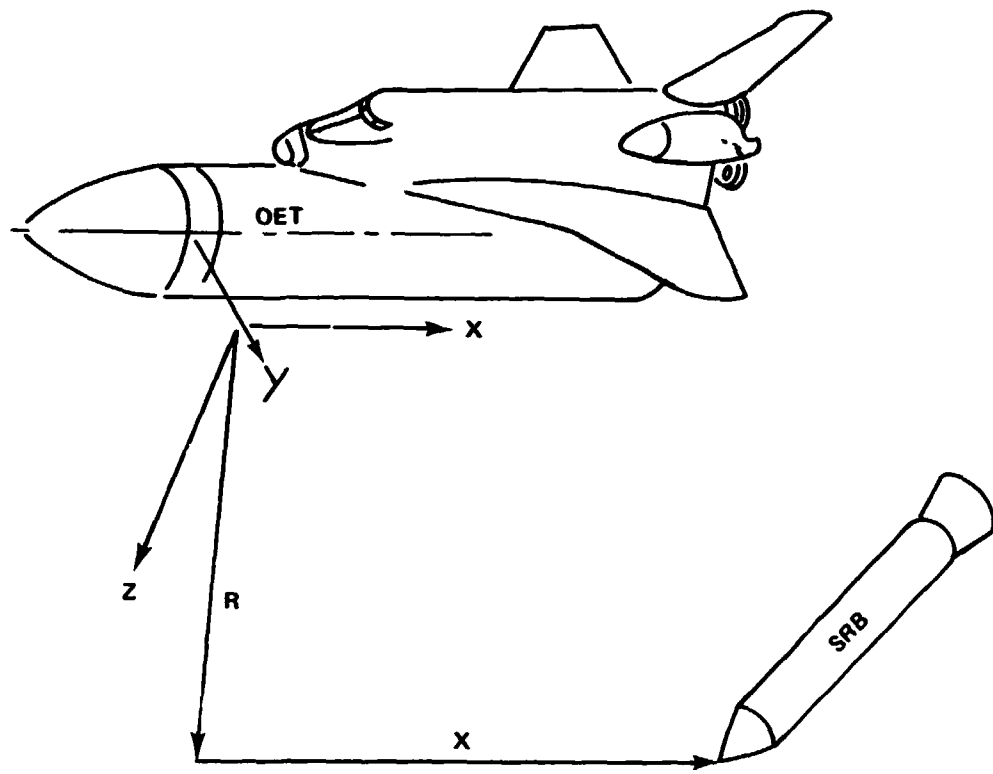
Figure A-3. Plume-on aerodynamics lookup variables.
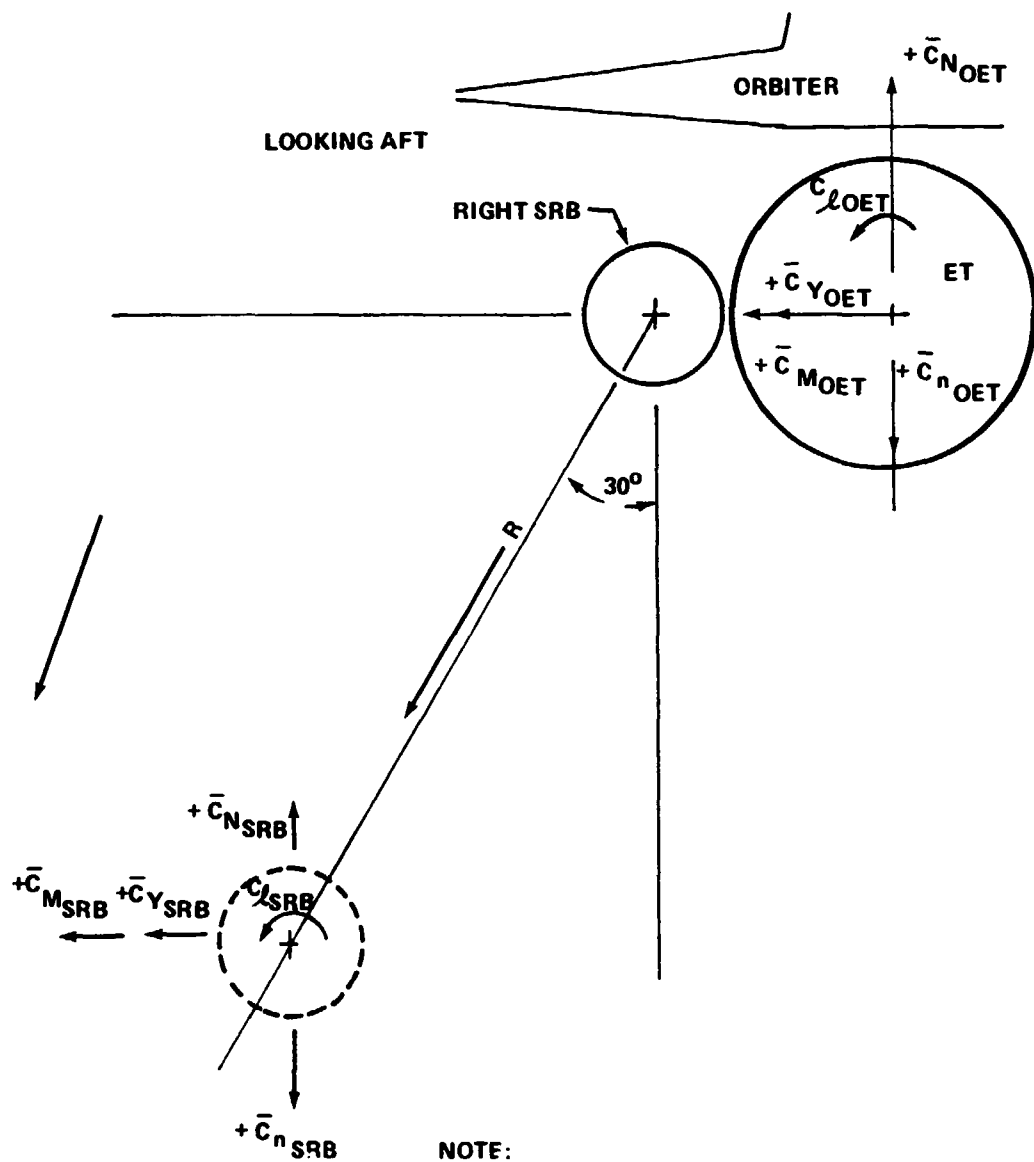
Figure A-4. Aerodynamic coefficient definition.

REFERENCES

1. Johnson Space Center, April 1975: Space Shuttle Program Level II
    Specifications, 07700, Vol. X.

2. Tomlin, D. D., January 7, 1975: Booster Separation Motor (BSM)
    Alignment Tolerance, MSFC Memorandum ED13-74-37.

3. Tomlin, D.D., June 23, 1975: SRB Bell Snubber Effects on Shuttle
    Control during SRB Thrust Tailoff, MSFC Memorandum ED13-44-75.

APPROVAL

SPACE SHUTTLE SOLID ROCKET BOOSTER (SRB) SEPARATION

by Donald D. Tomlin

The information in this report has been reviewed for security classification. Review of any information concerning Department of Defense or Atomic Energy Commission programs has been made by the MSFC Security Classification Officer. This report, in its entirety, has been determined to be unclassified.

This document has also been reviewed and approved for technical accuracy.

James C. Blair
Chief, Control Systems Division
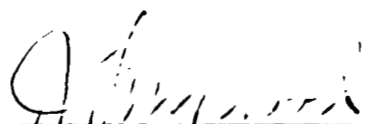
J. A. Lovingood
Director, Systems Dynamics Laboratory